Geomorphology 107 (2009) 178–194

Contents lists available at ScienceDirect

Geomorphology

journal homepage: www.elsevier.com/locate/geomorph

# Desert pavement development and landscape stability on the Eastern Libyan Plateau, Egypt

Katherine A. Adelsberger *, Jennifer R. Smith

*Washington University in St. Louis, Department of Earth and Planetary Sciences, One Brookings Dr., St. Louis, MO 63130, USA*

ARTICLE INFO

*Article history:*
Received 20 May 2008
Received in revised form 4 December 2008
Accepted 5 December 2008
Available online 16 December 2008

*Keywords:*
Desert pavement
Arid geomorphology
Middle Paleolithic
Upper Paleolithic
Egypt
Libyan Plateau

ABSTRACT

Desert pavement surfaces of the eastern Libyan Plateau in central Egypt represent a stable landscape preserving Middle and Upper Paleolithic artifacts. Detailed measurements of pavement clasts indicate significant variability in clast size, density, lithology and orientation between pavements, but no spatial relationship among any of these pavement variables over the study area. Pavement characteristics are unrelated to local geomorphic features including slope gradient and aspect, suggesting a desert pavement surface that has developed without significant influence from transporting mechanisms such as overland flow and slope failure. Meridional vertical cracks in surface clasts implicate thermal stresses due to diurnal solar variation as a mechanical weathering process, whereas the presence of a clast-free silty layer within all soil profiles indicates that these are accretionary pavement surfaces that have grown upward over time. The desert pavement in this region has likely developed *in situ* through mechanical breakdown of surface clasts and desert pedogenesis, indicating long-term stability for this region and minimal taphonomic effects on artifacts >2 cm in diameter deposited on this surface over the last ca. 100 ka.


## 1. Introduction

The Abydos Survey for Paleolithic Sites (ASPS) has been conducting a systematic surface survey of the eastern Libyan Plateau near Abydos, Egypt since 2000 (Fig. 1). The unexpectedly rich Middle and Upper Paleolithic record preserved in this high-desert environment, representing periods of hominin activity during the last 140,000 years (Chiotti et al., 2007), has the potential to inform models of desert occupation that could serve as a comparison to landscape use in the nearby Nile Valley (Olszewski et al., 2005). However, the almost exclusively surface context of these artifacts necessitates a thorough understanding of desert pavement formation and developmental processes in order to recognize possible depositional and taphonomic effects on archaeological materials. Site-scale examination of desert pavements on the Libyan Plateau performed as part of the ASPS survey focused on both surface and subsurface characteristics of these pavements in order to clarify the relationship between archaeological materials and their depositional setting.

Both archaeological and geomorphological work in arid zones often involves a primary focus on surface contexts, in which the dating and correlation of different desert surfaces can be difficult (e.g., McFadden et al., 1989). Because they are common arid zone landforms (Cooke and Warren, 1973), desert pavements are often the focus of arid landscape studies. Desert pavements can also be useful relative age indicators, as the comparison of desert pavement morphology (Al-Farraj and Harvey, 2000) or desert varnish development (Dorn and Oberlander, 1982) may offer one of the only feasible *in situ* methods for determining the relative ages of desert surfaces such as river terraces and alluvial fans. Other potential taphonomic information can be obtained from desert pavement surfaces, including the potential for lateral transport of surface clasts as well as downward movement of artifactual materials. Once the transport processes acting on any given desert pavement clast are known, more reliable behavioral interpretations can be made using artifacts obtained from these desert pavement surfaces. Understanding archaeological context begins by understanding the pavement formation and landscape stability of the region in question.

The Libyan Plateau of Central Egypt is currently a hyperarid environment, as even the nearest Nile Valley cities receive less than a millimeter of rainfall per year on average (Shahin, 1985). This area has probably been an arid region since the early Holocene, when pluvial conditions were last present in North Africa (Szabo et al., 1995; Hoelzmann et al., 2001). A more significant humid period also occurred across the Sahara ca. 120–140 ka (e.g., Gaven et al., 1981; McKenzie, 1993; Smith et al., 2004); these wetter conditions may have encouraged the use of the Libyan Plateau by Middle Paleolithic groups, and would explain the presence of earlier artifact assemblages in this currently uninviting environment. Pluvial events likely served as the primary control on the timing of human occupation in the high desert environments of Egypt (Chiotti et al., 2007).

In most places the Libyan Plateau is capped by the Eocene Thebes Group limestones (Said, 1990); in the study area examined here this cap is

* Corresponding author. Current address: Knox College, Department of Environmental Studies, Two East South St., Galesburg, IL 61401, USA. Tel.: +1 309 341 7274; fax: +1 309 341 7718.
*E-mail address:* kadelsbe@knox.edu (K.A. Adelsberger).

0169-555X/$ – see front matter © 2008 Elsevier B.V. All rights reserved.
doi:10.1016/j.geomorph.2008.12.005

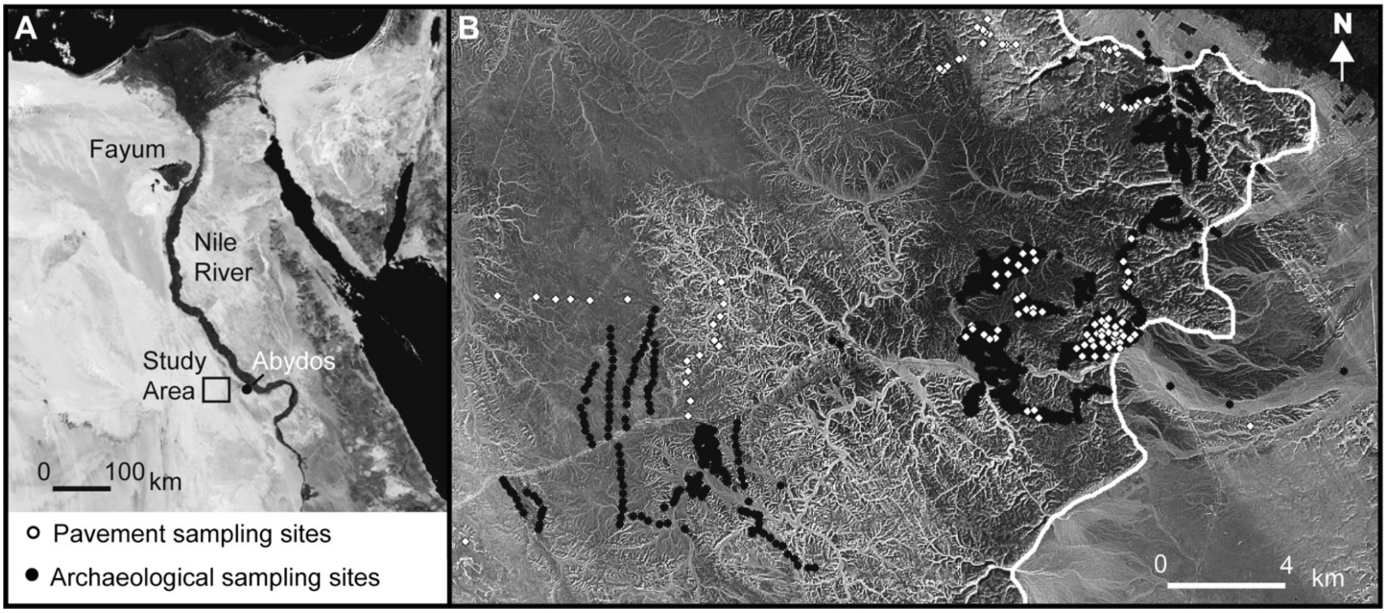


**Fig. 1.** A. Abydos Survey for Paleolithic Sites field area illustrated over MODIS imagery of Egypt, image credit Jacques Descloitres, MODIS Land Science, courtesy of Team Visible Earth (http://visibleearth.nasa.gov/). B. Pavement and archaeological sampling locations shown against satellite imagery of the eastern Libyan Plateau. The Nile Valley is the dark low area to the east; plateau edge is outlined in white.

composed of the Drunka and Serai Formations of the upper Thebes Group (Klitzsch et al., 1987). Given that rates of granite weathering in the climatically similar Central Namib Desert exceed 30–80 cm per 100 ka (Cockburn et al., 1999), surface lowering in areas of the Libyan Plateau where limestone bedrock is exposed has probably averaged more than a meter per 100 ka. However, plateau surfaces here are almost uniformly covered by desert pavement, with very little post-Eocene sedimentary deposition other than limited soil formation and localized deposition of "old" (undifferentiated Oligocene to Pleistocene (Klitzsch et al., 1987)) gravels. The uniform nature of the pavement surface present here and the lack of significant post-Eocene sedimentation or erosion indicate widespread stability of the soil horizons present. Surface lowering has probably been limited to unprotected (pavement-free) surfaces, whereas sediment accumulation occurs only where the surface gravels produce sufficient surface roughness to serve as a dust trap (e.g., Dong et al., 2002). These processes limit sediment removal and accumulation, as they both require significant geologic timescales to effect significant change on a landscape; the plateau surface has probably remained relatively unchanged since Middle Paleolithic times (140–40 ka (Chiotti et al., 2007)).

The majority of Quaternary erosion in this region would have occurred along the edge of the escarpment and as headward erosion within drainages, as is apparent in the modern landscape. Wadi downcutting and headward erosion has resulted in isolated plateau surfaces connected by narrow ridges separating opposing wadi heads. The result of these erosional patterns is a modern plateau surface incorporating significant topographic variation, where wadi-facing slopes may be significant (measuring up to 10–15°in the field). The modern plateau has therefore evolved from a much less dissected landscape, and further headward erosion may lead to completely isolated plateau surfaces in some areas. Wadis in the study area are often composed of numerous straight stretches oriented NE–SW and NW–SE (Fig. 1). This rectangular drainage pattern indicates structural (jointing) control on the formation of drainages in this area (Howard, 1967).

### *1.1. Desert pavements and desert surface geomorphology*

Desert pavements are generally characterized by a surface layer of coarse clasts overlying finer sedimentary units (McFadden et al., 1987). The specific characteristics of pavement surfaces are often described through measurement of individual clasts, the determination of overall grain size and sorting, and a measure of overall clast coverage on a given surface (e.g., Poesen et al., 1998; Al-Farraj and Harvey, 2000). These measurements may provide an indication of the relative ages of desert surfaces, where decreasing clast sizes and increased coverage by smaller clasts indicate older pavement surfaces (Al-Farraj and Harvey, 2000). Clast coverage may also vary with slope gradient due to spatial variation in the depositional and erosional history of particular desert slopes. In these cases, both coverage and size of fragments increase as slope gradient increases (Poesen et al., 1998), resulting in larger clasts on steeper slopes.

Clast lithology can affect pavement formation, since lithologies more susceptible to weathering processes will break down more quickly into smaller pieces (Poesen et al., 1998; Al-Farraj and Harvey, 2000; Allison et al., 2000). Clast coverage, while related to landform development itself, is probably not directly influenced by clast lithology (e.g., Poesen et al., 1998). However, coverage may control infiltration, underlying soil development and the location of vegetation within an arid landscape. Pavement surfaces will prevent infiltration, leading vegetation to prefer (and disturb) more open areas in a pavement landscape (Wood et al., 2005). The presence of vegetation may in turn prevent erosion on hillslopes, leading to lowered rates of pavement formation on those slopes (Poesen et al., 1998). The measurement of pavement clasts and the percent coverage of desert pavement surfaces may elucidate the primary controls on desert landscape development by revealing the relationships between lithology, clast size, slope and coverage.

The soil profile underlying many desert pavement surfaces consists of a vesicular A (Av) horizon (Cooke, 1970; Dixon, 1994; McFadden et al., 1998), which may develop through repeated cycles of wetting and drying and entrapment of air within silty sediments at the surface (Miller, 1971; Nettleton and Peterson, 1983). The development of a vesicular layer is dependent upon the accumulation of aeolian silts and clays, which would trap air during seasonal shrinking and swelling (Wells et al., 1985; McFadden et al., 1986, 1987). Beneath the Av horizon is a relatively gravel-free B horizon, which may be similar in composition to the A but lacks the vesicular nature of the Av. In some cases the nature of underlying soil horizons may influence overlying pavements; vertical cracking and shrink/swell actions within Vertisols may move clasts toward the surface (e.g., Moeyersons et al., 2006). Regardless of underlying soil composition, more mature pavements tend to have a smoother surface expression and a more interlocking pavement surface (Al-Farraj and Harvey, 2000) as well as a thicker and less gravelly B horizon (Amit et al., 1993).

Models of desert pavements as deflated gravel lags (e.g., Summerfield, 1991) or as the result of upward migration of coarse gravels due to the shrinking and swelling of finer-grained soil horizons (e.g., Cooke, 1970) have been replaced in some cases by the accretionary model developed by McFadden et al. (1987). Some pavements are now thought to form *in situ* through the deposition of fine-grained aeolian sediment, which accumulates beneath and maintains a layer of coarse material at the surface (Wells et al., 1985; McFadden et al., 1986, 1987; Wells et al., 1995). In the absence of dateable surface materials, the evidence for accretionary pavement formation would be largely subsurface, where a clast-free zone of fine eolian sediment would be present instead of a mixture of coarse and fine (wind-removable) sediments.

The fabric of pavement surfaces is largely controlled by slope gradient (e.g., Abrahams et al., 1990). Clasts on arid slopes tend to be oriented with their long-axes parallel to the downslope direction, most likely due to hydraulic activity (Abrahams et al., 1990) or creep (Mills, 1983). In desert environments local hydrology may vary significantly over small areas, leading to increased runoff and variations in surface characteristics on slopes of particular aspect due to microtopography at the surface and the variable susceptibility of different surfaces to rill formation even when local bedrock is homogenous (Yair et al., 1980). Variations in local overland flow may therefore account for non-uniform clast orientation over even small areas of the same slope.

Fabric may be more pronounced on steeper slopes (Mills, 1983), as the movement of clasts can be dependent upon both clast size and slope gradient (Frostick and Reed, 1983). Gradient and aspect may also control the degree of clast coverage and the sorting of clasts on arid or semiarid slopes, with coarser materials present in some areas due to variations in erosion and deposition (Poesen et al., 1998), which can also vary significantly within a small local area (Reid and Frostick, 1985). The rates and likelihood of clast movement on slopes may also be increased significantly when exposed to anthropogenic activities, particularly trampling by livestock (Nyssen et al., 2006). Given all of these controls on pavement fabric, a consistent relationship between

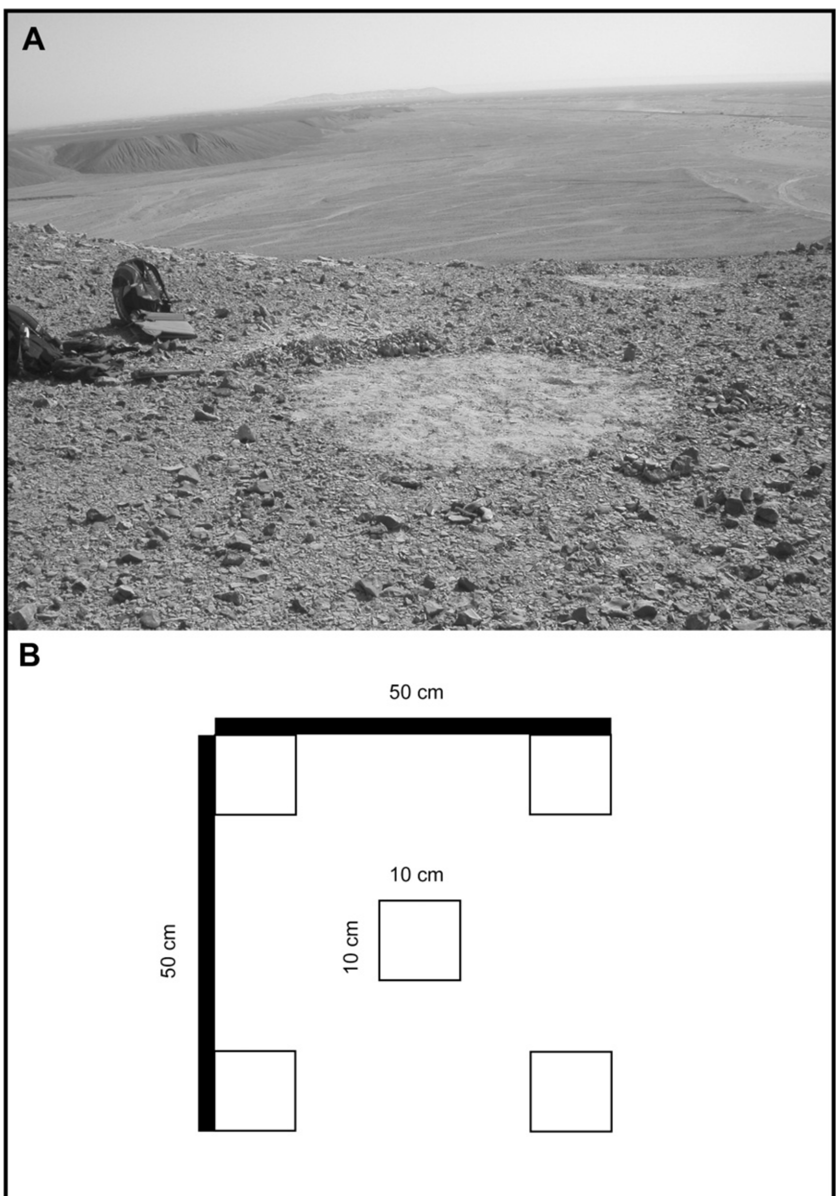


**Fig. 2.** A. Cleared archaeological sample circle after sampling, field packs for scale. B. Sketch of 0.25 $m^2$ pavement sample area (defined by 0.5 m wooden edge guides) illustrating common areas of clast counts within 100 $cm^2$ squares inside each sample.

**Table 1**
Comparison of pilot season data and the subset of clasts represented in Table 2.

| | Chert | | Limestone | | Quartz | | Calcite |
|---|---|---|---|---|---|---|---|
| | Pilot | Full | Pilot | Full | Pilot | Full | Pilot |
| Average area | 7.54 | 2.45 | 8.17 | 1.63 | 3.32 | 1.24 | 3.07 |
| Average length/width | 1.63 | 1.47 | 1.56 | 1.34 | 1.44 | 1.26 | 1.50 |
| *n* | 1483 | 2235 | 893 | 315 | 121 | 460 | 3 |

Average clast sizes obtained by random selection of fifty clasts (pilot) are significantly larger than those obtained by full counts of small sample areas (full), whereas length/width ratios are more similar. $\rho=0$ for all two-sample Student's *t*-tests comparing both individual clast area and length/width ratios.

size or orientation of clasts and gradient may not occur in all arid areas. However, considering the significant slopes present on the modern Libyan Plateau, the formation of desert pavements during the Quaternary (as well as the positions of any archaeological materials associated with these surfaces) may have been influenced by the presence of slopes.

Although well-known as stable landscape features, desert pavements are easily disturbed (Ward, 1961), and lateral movement of clasts may serve to "heal" areas of disturbance (Cooke, 1970) over a period of only decades (Prose and Wilshire, 2000). In some cases the creep associated with pavement healing may occur over distances of several centimeters (Haff and Werner, 1996), indicating that pavement clasts are capable of significant lateral movement. However, clast movement in undisturbed pavements is probably minimal, on a scale of only several millimeters even where pavement is subject to rainfall events and overland flow (de Ploey and Moeyersons, 1975). Lateral movement of clasts may therefore occur even in the absence of significant slopes, changing the orientation and position of pavement clasts at the surface. Creep and non-slope-related effects should be considered in any study examining pavement fabric.

This study investigates the clast-scale characteristics of desert pavements in an effort to recognize the primary developmental controls (e.g., slope, bedrock, soil formation) on pavement variation by identifying existing relationships between surface clast characteristics (e.g., size, coverage, lithology) and regional landscape features (e.g., slope, bedrock). The orientation of clasts along slopes and correlation of clast orientation with slope steepness would support slope-controlled (overland flow, gravity-driven processes) influences on pavement development (e.g., Reid and Frostick, 1985), whereas the recognition of a subset of pavement surfaces containing significantly smaller clasts or more open pavements may indicate different ages of formation for portions of the pavements in question (Al-Farraj and Harvey, 2000). A clast-free soil horizon beneath pavement surfaces would support an accretionary developmental model (Wells et al., 1985; McFadden et al., 1986, 1987; Wells et al., 1995), whereas orientation of clasts may indicate lateral transport of surface clasts (Mills, 1983). Understanding these aspects of pavement development during the Quaternary will clarify the taphonomic history of artifacts found on the plateau during archaeological surface survey, which will in turn inform the reliability of behavioral interpretations based upon these assemblages.

## 2. Methods

Desert pavement surfaces were analyzed adjacent to archaeological sample localities in order to characterize the pavements most relevant to potential taphonomic issues in the archaeological record. During archaeological survey, samples were taken from circles one meter in radius at 100-meter to 250-meter intervals across the survey area (Fig. 2A); archaeological site samples were also taken wherever artifacts were found in dense concentrations (sites) between sampling points. Because time constraints prohibited geologic analysis of every archaeological sample, geologic studies of pavement surfaces were carried out on a less regular and wider spacing in an effort to characterize pavements throughout the study area (Fig. 1). Pilot season data from the winter of 2002/03 revealed that random selection of clasts along circle margins led to a bias toward larger clasts (Table 1); random selection was therefore avoided during pavement sampling.

Each pavement surface was photographed as a 0.25 $m^2$ section (this section will be referred to as a "sample") with one edge oriented N–S (after Poesen et al., 1998; Al-Farraj and Harvey, 2000). Within each sample, 100 $cm^2$ areas (referred to as "squares") were defined to obtain representative subsamples of the pavement surface (Fig. 2B). Lithology and maximum length to the nearest half centimeter, measured with a measuring tape, were recorded for all clasts found

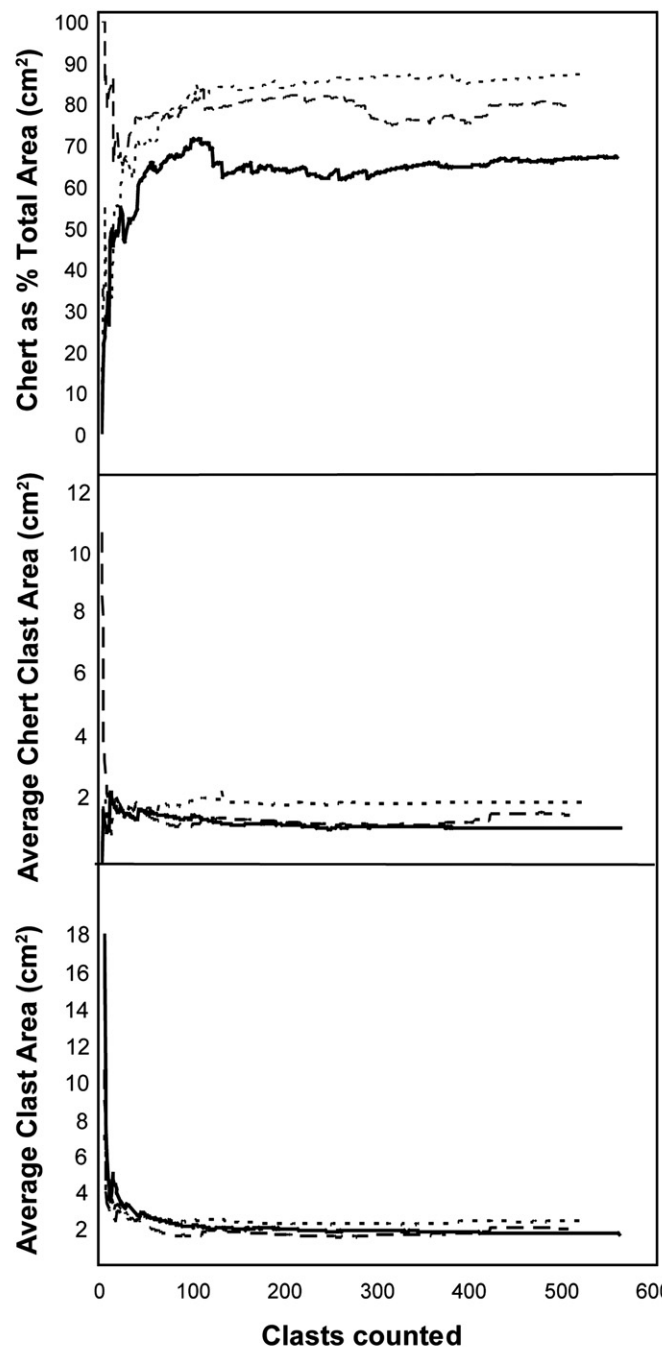


**Fig. 3.** Results of three long-count samples illustrating the number of clasts that must be counted in order to obtain representative measurements for the pavement sample as a whole.

at the surface. Pavement clasts included in the counts were not incorporated into the underlying soil horizon and were freely removable from the underlying clast-free silt. This method of measurement allowed for faster collection of field data without reducing the value of the data collected, as mm-scale variation in the diameter of coarse gravels has less geomorphic and depositional significance than similar variation among sandy sediments (Briggs, 1977). Data from additional squares were collected in the same manner until 100 clasts had been counted (Fig. 2B). Once a count of 100 clasts was reached, all clasts were counted within the current square before ending the sample. Finishing counts within squares allowed for a more accurate determination of the density of surface clasts on both inter- and intra-sample scales, as the densities of individual squares could be calculated in addition to the density of the sample as a whole. One hundred clasts was used as the minimum count following “long counts” of 500+ clasts within a sample to determine the point at which the data collected represented the pavement lithology and clast density in the immediate area (Fig. 3). A total of 16,392 clasts were measured in this manner from 120 individual sites.

Measurement of both maximum (length) and maximum measurement perpendicular to length (width) surface dimensions of 5510 clasts allowed for the determination of average length/width ratios for chert, quartz, calcite and limestone clasts in regional desert pavement surfaces (Table 2). These numbers were later used to estimate the average surface area of clasts when only the maximum length had been measured in the field. This method of data collection allowed us to expedite field measurements and sample a larger number of clasts over a larger portion of the study area. Surface area of clasts provides a reliable comparative measure of clast coverage because, although the orientation of clasts relative to the ground surface may vary (e.g., split fragments versus primary material), the majority of clasts within desert pavements lie with their long-axes parallel to the ground surface (Cooke, 1970). These length/width data were also used to calculate surface coverage of pavement clasts within squares (see Appendix).

Although pilot season data indicated that random selection of clasts led to the measurement of larger clasts on average than did the sampling methodology used in this study, it is likely that the methods used here still led to a size bias, this time against the identification of large boulders within the study area. When selecting 0.25 $m^2$ areas for pavement counts, wooden guides were placed as parallel as possible to the modern surface, and large boulders were avoided in order to provide pavement samples that were most relevant to artifact taphonomy and which could provide the 100-count minimum required for accurate regional characterization (Fig. 3). Boulder avoidance required no more than one meter of lateral adjustment of our sampling area, and probably had little effect on the data obtained for smaller pavement clasts. These counts are therefore a more accurate means of characterizing small-scale pavement characteristics, but may under-represent the proportion of larger (>0.25 $m^2$) boulders within the study area. Observations of local surface geology were made in an effort to identify those pavements found in regions containing larger numbers of boulders, but boulder-distribution was not specifically relevant to the aims of this study.

Where vertical cracks were present in surface clasts, their orientations were measured using a Brunton compass corrected to the current magnetic declination of 3°E. The locations of measurement sites were recorded using hand-held GPS units and described qualitatively in terms of slope (flat, gentle, moderate or steep) and slope direction (N, NW, S, etc.). Orientations of pavement clasts were determined on a subset of 27 pavements by drawing straight long-axis (maximum measurable dimension) orientations of individual clasts on photographs of pavement samples taken parallel to ground surface and corrected for photographic distortion using ArcGIS 9.2. Orientations were drawn on all clasts where a long-axis could be identified. Resulting vector directions were exported as degrees to correspond with Brunton measurements made in the field. The results of both of these vector analyses were plotted as non-polar frequency lines in 10-degree bins within full-circle rose diagrams, and circular statistics were evaluated using GEOrient 9.2. Statistical values reported by this program are based on Fisher (1993) and Mardia and Jupp (1999). Vectors determined from pavement photographs were weighted equally regardless of clast size. These data may be biased in that the orientations determined are preferentially on larger clasts as well as those found closest to the modern surface within the pavement, as the overlap of clasts makes it difficult to determine clast orientation for all clasts from photographic evidence. Therefore, more open pavements as well as those with larger clasts are more likely to provide more accurate orientation data; however, all data presented here were determined through the same method by the same observer.

In addition to surface clast measurement and sampling, we excavated 97 small pits to gravel or limestone bedrock. Profiles of these pits were described in terms of pavement thickness, subsoil thickness, A-horizon development and consolidation, presence or absence of salts, and presence or absence of subsurface clasts. Pits were placed on a variety of pavement types (varying in primary lithology and density of surface clasts) as well as a number of different slopes (varying in slope direction and degree). All mapped points were recorded using hand-held GPS units. Additional geomorphic data (slope, aspect, elevation) were extracted from a (30 m) Advanced Spaceborne Thermal Emission and Reflection Radiometer (ASTER) Digital Elevation Model (DEM). However, these DEM data average 30 m per pixel, representing a much coarser scale than that of the data collected in the field. In order to provide a more spatially accurate means of comparing slope variation with pavement characteristics, each pavement was assigned a more qualitative “index” of gradient based upon field observations, where 0 = flat, 1 = gradual, 2 = moderate and 3 = steep (see Appendix). There is only a very weak positive correlation between qualitative slope indices and DEM-derived slope values (uncorrected Spearman rank order correlation 0.14, $t = 1.02$ (Wessa, 2008)) (Table 3). The fact that the steepest slope extracted from the DEM, 22°on sample 07PV49, received only a “moderate” slope index (Appendix) indicates that these extracted data are indeed less than representative of the actual slope affecting a given pavement surface. Spatial statistics (Morans I spatial autocorrelation) were run

**Table 2**
Length/width ratios of pavement clasts divided by lithology.

| | Chert | Limestone | Quartz |
|---|---|---|---|
| Average | 1.47 | 1.34 | 1.26 |
| Stdev | 0.53 | 0.44 | 0.38 |
| *n* | 2235 | 315 | 460 |

**Table 3**
Spearman rank order correlation for slope indices (calculated using Wessa (2008)) versus pavement characteristics (Spearman, 1904).

| | *R* (uncorrected) | *R* (corrected) | *t*-test | *Z* score | *n* |
|---|---|---|---|---|---|
| # Chert clasts | 0.11 | 0.07 | 0.72 | −1.23 | 116 |
| % Chert | 0.11 | 0.08 | 0.82 | −1.32 | 116 |
| Average area | 0.10 | 0.05 | 0.54 | −1.06 | 116 |
| Median area | 0.14 | 0.05 | 0.54 | −1.52 | 116 |
| Stdev area | 0.09 | 0.04 | 0.42 | −0.94 | 116 |
| Burial | 0.22 | 0.17 | 1.88 | −2.31 | 115 |
| Density | 0.16 | 0.11 | 1.23 | −1.71 | 115 |
| Slope (DEM) | 0.14 | 0.10 | 1.02 | −1.51 | 115 |
| Elevation | 0.01 | −0.05 | −0.49 | −0.08 | 115 |
| Aspect | 0.17 | 0.12 | 1.29 | −1.77 | 115 |
| Pavement orientation (kappa) | 0.11 | 0.08 | 0.37 | −0.54 | 25 |

Spearman rank correlation (*R*) values near −1 indicate negative correlation, 0 indicate no correlation, and 1 indicate positive correlation. *n* value indicates number of pairs tested in each case.

**Table 4**
$R^2$ values for linear regressions for pavement measurements and potential geomorphic controls and von Mises–Fisher distribution kappa values for pavement orientations.

| | Burial | Slope (DEM) | Aspect | Kappa |
|---|---|---|---|---|
| # Chert clasts | 0.05 | 0.02 | 0.00 | 0.08 |
| % Chert | 0.05 | 0.00 | 0.00 | 0.00 |
| Average area | 0.39 | 0.03 | 0.01 | 0.12 |
| Median area | 0.17 | 0.00 | 0.00 | 0.07 |
| Stdev area | 0.30 | 0.03 | 0.01 | 0.03 |
| Burial | – | 0.10 | 0.00 | 0.02 |
| Density | 0.14 | 0.04 | 0.02 | 0.02 |
| Slope (DEM) | 0.10 | – | 0.02 | 0.08 |
| Elevation | 0.13 | 0.14 | 0.03 | 0.05 |

Data, calculations, units and definitions from Appendix.

using ArcGIS 9.2 in order to evaluate potential clustering in these datasets.

## 3. Results

### 3.1. Pavement characteristics

#### 3.1.1. Clast size and density

Pavement maturation is generally measured by an increase in clast coverage, a decrease in clast size, and an increase in the thickness of soil horizons (Al-Farraj and Harvey, 2000). We determined measures of clast size (surface area), clast burial (total clast surface area/surface area of pavement measured) and clast density (number of clasts measured per surface area of pavement analyzed) using values obtained in the field (Appendix), which can be used to compare the relative maturity of these pavement surfaces. Measures of clast density and burial in these pavements cannot be separated into distinct groups, suggesting that pavements examined here are developed to similar extents. Clast density and clast size are often linked to both pavement maturity (Al-Farraj and Harvey, 2000) and arid hillslope processes, where increased gradient and gravity-driven transport lead to size sorting and variations in clast coverage (e.g. Poesen et al., 1998). On the Libyan Plateau these measurements are unrelated to local geomorphologic characteristics including slope direction (aspect) and gradient (Tables 4). Because values extracted from the DEM represent an averaged area much larger than that relevant to the sampled pavements, we also compared pavement characteristics to semi-quantitative slope indices (Table 3, Appendix) and found no significant relationship (only slightly positive rank correlations) between any pavement characteristics and these index values.

The lack of correlation of pavement maturity indices (clast burial and density) with any potential expression of geomorphic control (slope, aspect, elevation) (Tables 3, 4, Appendix) suggests that geomorphic changes such as slope retreat or gravity-driven clast movements have not been the primary control on pavement formation during the Quaternary. In order to test whether variations in the local landscape have determined similar variations in pavement characteristics, we used Moran's Index spatial autocorrelation to determine whether the characteristics of adjacent pavements are more similar to each other (clustering in the data) (Moran, 1950). We would expect significant positive autocorrelation indices when characteristics such as clast density are controlled by spatially autocorrelated landscape features such as slope, drainage proximity, or sub-regional bedrock characteristics. Moran's I values close to zero indicate no spatial autocorrelation (no similarity between adjacent pavements),whereas values closer to 1 are more significantly positively spatially autocorrelated and values closer to −1 are more significantly negatively spatially autocorrelated (Moran, 1950). $Z$ values indicate degree of deviation, where a 95% confidence interval of randomness is indicated by $Z$ values between −1.96 and 1.96; values outside this range indicate statistically significant non-random distribution. The values determined here are positive but close to zero, indicating largely random distribution for some pavement characteristics but spatial autocorrelation for lithology, burial, and clast size (Table 5).

The strongly significant autocorrelation for landscape characteristics indicated by Moran's I $Z$ values is expected: slopes are steeper at the escarpment edge as well as along wadi cuts, and elevation is higher and more similar between sites as we move west within the study area (Fig. 1). Pavement characteristics that are controlled by these landscape features should therefore also be spatially autocorrelated. $Z$ values for pavement characteristics indicate clustering of clast burial and clast size, which are also the only correlated values observed by linear regression ($r^2=0.39$ burial vs. average size, $r^2=0.30$ burial vs. stdev size, Table 4). This linear relationship is not surprising, as burial is likely a function of size; field observations indicated that smaller clasts often cluster beneath the edges of larger clasts in interlocking pavements. Pavements with larger clasts on average and a corresponding increase in clast burial are found primarily in the eastern portion of the study area (Fig. 4). This may be due to the exposure of bedrock units to the east providing locally weathered materials, whereas many of the pavements in the western portion of the study area are formed on transported gravel deposits (Fig. 4).

#### 3.1.2. Clast lithology

Although linear regression indicates that slope and aspect are not directly related to clast lithology, burial or density (Table 4), these pavement characteristics may be related to the greater susceptibility of clasts of particular lithologies to erosion, which would in turn correlate with bedrock composition. Moran's I Z values indicate positive autocorrelation for lithologic composition within pavement surfaces (positive I, $Z>1.96$, Table 5), suggesting that lithology is being controlled by landscape features to some extent. The lithology of the pavement clasts is made up exclusively of four rock types: chert, limestone, quartz pebbles, and calcite crystals. Chert is the most common material found in these pavements, and is available as a weathering product from local bands within the limestone bedrock (Klitzsch et al., 1987). Chert cobbles are also a component of the Tertiary clastics and the undifferentiated Oligocene to Pleistocene gravel unit ("old gravel") (Klitzsch et al., 1987) mapped on the western edge of the study area (Fig. 4). Calcite crystals occur most frequently along the northern edge of the plateau, where calcite veins are frequently found at the surface. The lack of similar veins to the south and west account for the lack of calcite in other pavements studied here.

Because it is the major bedrock lithology in this area, limestone is a common component of pavements and occurs more frequently where bedrock is exposed, particularly along the eastern edge of the plateau (Fig. 4). Although quartz pebbles were frequently observed

**Table 5**
Morans I spatial autocorrelation results for pavement and geomorphic characteristics.

| | Moran's Index | Variance | $Z$ score |
|---|---|---|---|
| # Chert clasts | 0.15 | 0.00 | 2.75 |
| % Chert | 0.24 | 0.00 | 4.02 |
| Burial | 0.32 | 0.00 | 5.39 |
| Density | 0.05 | 0.00 | 0.88 |
| Average clast area | 0.17 | 0.00 | 3.92 |
| Median clast area | 0.13 | 0.00 | 2.31 |
| Stdev clast area | 0.01 | 0.00 | 0.25 |
| Slope (DEM) | 0.16 | 0.00 | 2.86 |
| Aspect | 0.03 | 0.00 | 0.69 |
| Elevation | 0.59 | 0.00 | 9.89 |
| Kappa | −0.08 | 0.00 | −0.61 |

$Z$ values indicate deviation; 95% confidence intervals lie between −1.96 and 1.96. $Z$ values above 1.96 indicate statistically significant clustering. Data, calculations, units and definitions from Appendix, except for kappa values which were used in Table 4.

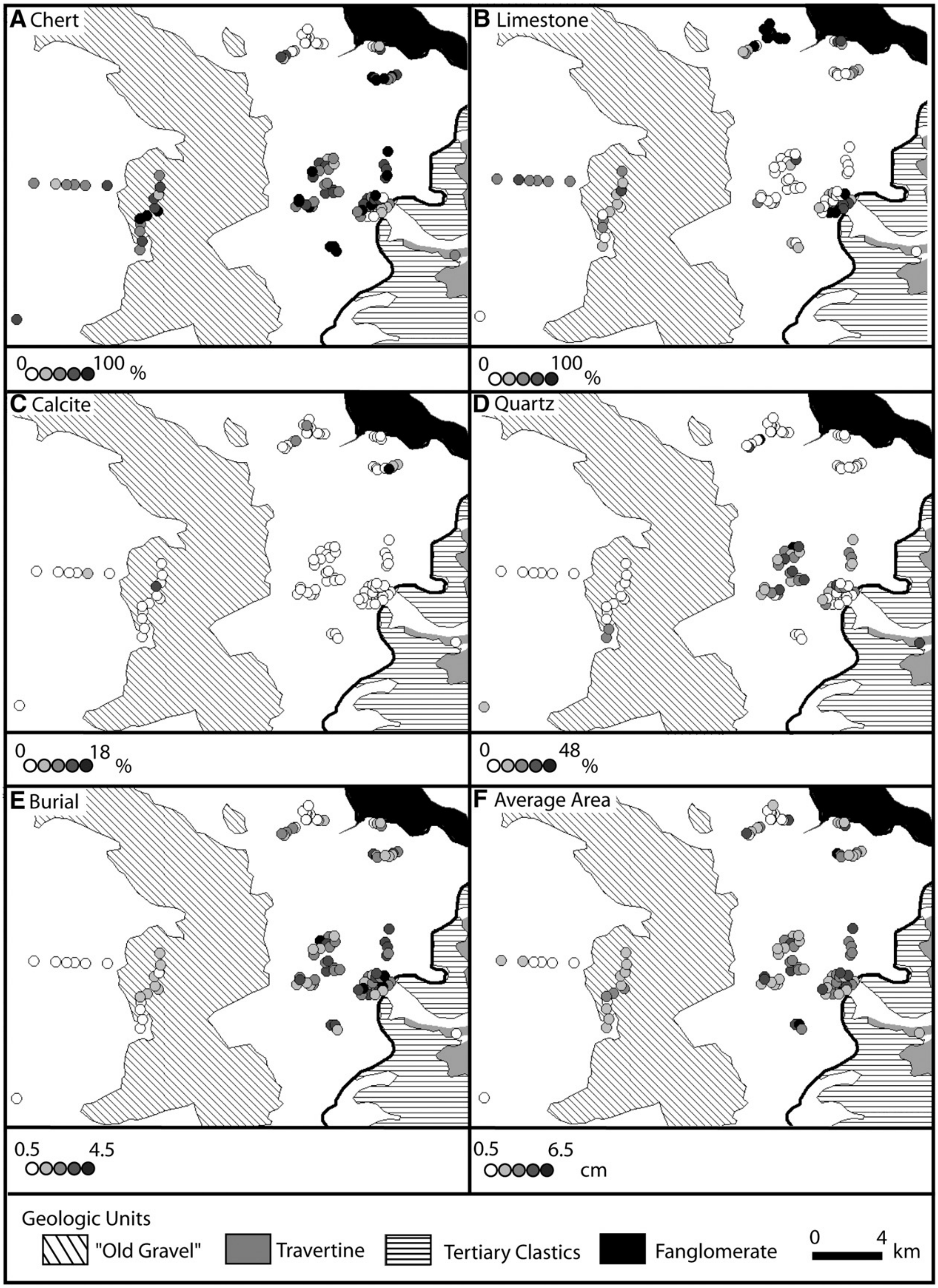


**Fig. 4.** Clast lithology at pavement sample sites illustrated as relative percentages (graduated colors, with higher percentages indicated by darker circles) for A. chert, B. limestone, C. calcite, and D. quartz. Clast burial and size also illustrated as relative values: E. burial index (dimensionless), F. average clast size (cm). Solid black line indicates the edge of the Plateau; the majority of sample sites occur on the Plateau (left of the line). The Nile Valley lowland lies on the right side of the figure. Local geologic units identified were mapped by Klitzsch et al. (1987). Fanglomerates, Tertiary Clastics and Travertines are all found at the foot of the Plateau and serve to designate the boundary between Plateau edge and Nile Valley lowland. Undesignated areas are underlain by Thebes Group limestones.

weathering out of undifferentiated gravels, the frequency of quartz pebbles in pavement surfaces is not directly related to the presence of the undifferentiated gravel. However, well-rounded quartz pebbles are found in all obviously transported gravel units. The distribution of quartz within pavement surfaces is presumably related to discontinuous patterns of gravel deposition; gravels were probably deposited as fluvial lags, which have since been deflated to form bedrock surfaces for more recent desert pavement development. The lack of a detailed geologic map illustrating the underlying bedrock facies present on the plateau makes it difficult to determine potential relationships between pavement lithology and bedrock composition with any certainty, but the autocorrelation of pavement lithology and the observed variation of clast composition with bedrock (e.g., presence or absence of calcite crystals) indicates a relationship between pavement lithology and bedrock as well as minimal long-distance transport of surficial materials.

The limestone plateau is composed of a number of different facies, including chert-bearing, bedded limestones and friable silty limestone

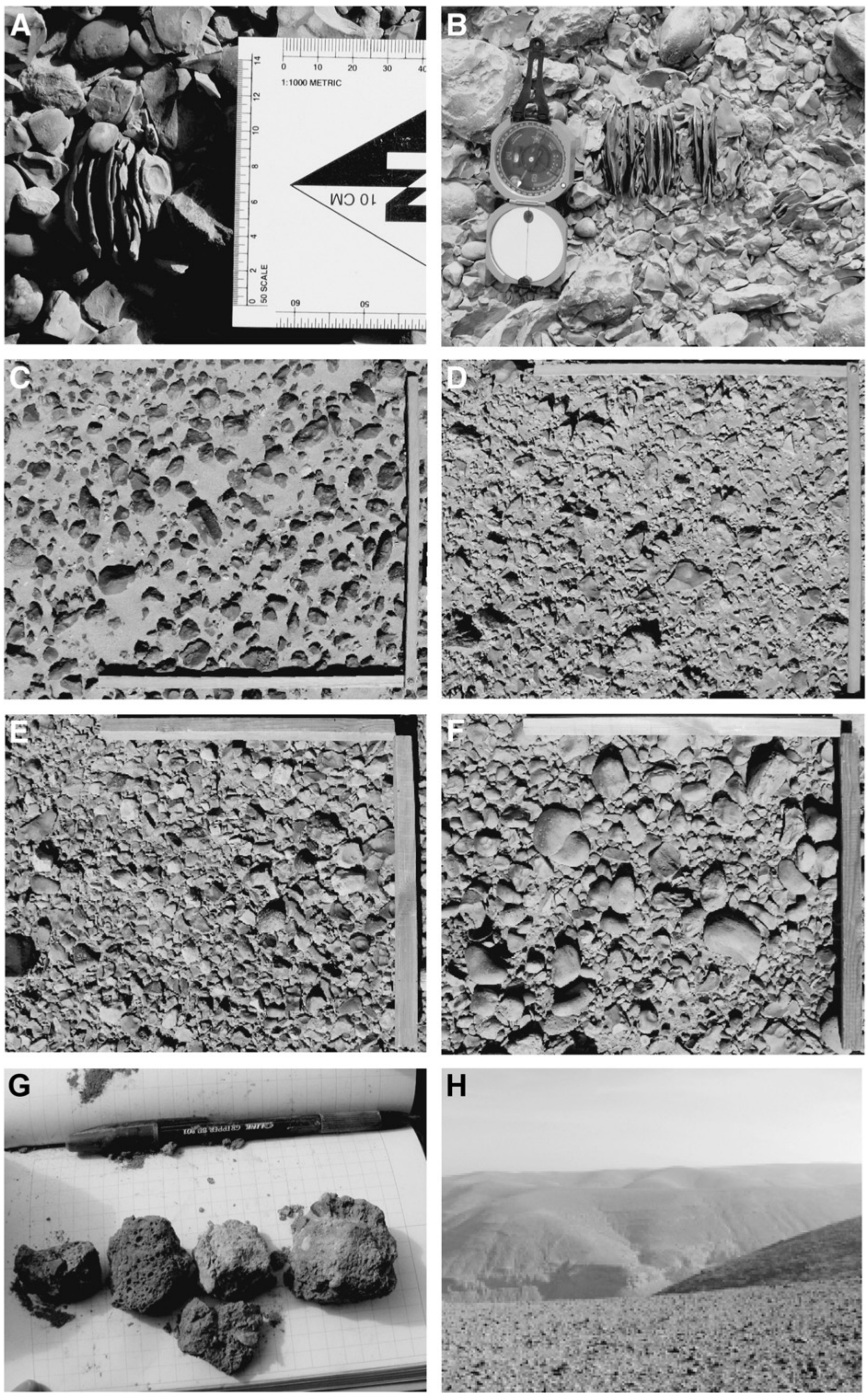


**Fig. 5.** Field photos from ASPS: A, B. Vertical cracks in surface chert clasts; C, D, E, F. Examples of pavement surfaces examined in this study. Wooden guides outline 0.50 m edges for each pavement sample. All clasts within the square outlined by the guides would be counted and measured (see Fig. 2B); G. Portions of Av horizons, illustrating vesicularity, presence of small clasts within the horizon and their consolidation. Displayed on field notebook, pen for scale; H. Field photo illustrating the nature of the landscape through much of the study area.

deposits, each of which may have a controlling influence on pavement lithology (i.e., percent chert or calcite) as well as the depth of soil formation and resistance to erosion. The lack of correlation between major pavement qualities and any obvious, measurable geomorphic characteristics suggests that differences in the chert content and resistance to weathering of locally variable bedrock facies played a major role in later pavement formation and development. The loose demonstrable relationship between pavement lithology and bedrock units, to the extent that these relationships can be made using our current understanding of bedrock lithology, as well as the lack of any indication of clast transport (e.g., no identifiable correlation between slope gradient and pavement development or clast size) suggest that soil and pavement formation in this area has been controlled by pre-existing bedrock conditions.

### *3.2. Erosional processes*

Parallel vertical cracks were observed in chert cobbles at a number of sites in the study area. These cracks were often parallel to the long-axis of the cobbles and always vertical where multiple cracks were present (Fig. 5). Measurement of parallel vertical cracks in surface clasts reveals a strong N–S preferential orientation of cracks on all pavement surfaces, within the range of "meridional" cracks (within 33° of N–S) defined by McFadden et al. (2005) for the majority of the data (Fig. 6, Table 6). The estimated kappa ($\kappa$) value obtained by the von Mises–Fisher distribution for the entire dataset is 0.30, where $\kappa > 0$ indicates unimodal distribution, higher $\kappa$ values indicate more concentrated data and $\kappa = 0$ indicates uniform (random) distribution of the data (Mardia, 1975; Fisher et al., 1987). Although variances for these data are relatively high, $\kappa$ values indicate unimodal distribution and a higher level of preferred orientation for cracks than for any pavement clasts examined elsewhere in this study.

The N–S orientation of the measured cracks (Fig. 6, Table 6), suggests mechanical weathering due to thermal stresses caused by diurnal solar variation, following McFadden et al. (2005). Although these cracks were not observed in all parts of the study area, their presence solely in chert cobbles suggests that chert is more susceptible to cracking, potentially due to its dark color (Summerfield, 1991), shape, size, or other physical properties that would enhance thermal stresses within a chert cobble. The presence and size of chert cobbles within local pavement surfaces may therefore determine the presence or absence of vertical cracks (Fig. 6).

Solar-controlled mechanical weathering is probably acting to break down clasts at the surface by forming the initial (thermal) cracks. Additional processes such as salt weathering (e.g., Amit et al., 1993), frost shattering or hydration shattering (e.g., Summerfield, 1991) may play a role in further breakdown and shatter of these clasts by widening the initial thermal cracks. The occurrence of thermal cracking, salt weathering, hydration shattering and freeze-thaw action on the Plateau suggests that clast breakdown could occur *in situ,* and pavements may not have been dependent upon additional processes, such as transport or trampling, for the development of smaller and more numerous clasts over time. Thermal cracking would play a role in the breakdown of larger clasts, but thermal processes would have little effect upon clasts too small to develop significant thermal gradients (McFadden et al., 2005). This minimum size limit for thermal cracking may determine a minimum clast size for these pavements, as thermal shattering (and in turn other mechanical processes) would have no effect upon pavements below a particular size threshold.

### *3.3. Pavement fabric*

Orientations of surface clasts within full 0.25 $m^2$ sample areas were determined from digital photographs taken parallel to the ground surface (Fig. 5). Orientations obtained for these pavements have been quantified as estimated $\kappa$ values obtained by von Mises–Fisher distribution (Mardia, 1975), where larger $\kappa$ values indicate less variance in the data (Table 6). In arid environments, surface clasts are often oriented on slopes where hydraulic activity or creep has played a role in clast movement (e.g., Mills, 1983; Abrahams et al., 1990). However, comparison of $\kappa$ values for the pavement samples examined here with both geomorphic and pavement characteristics indicate no relationship between pavement orientation and any other measured characteristic ($r^2 \leq 0.12$ for all comparisons) (Table 4). Some pavements are oriented to varying degrees, whereas others contain

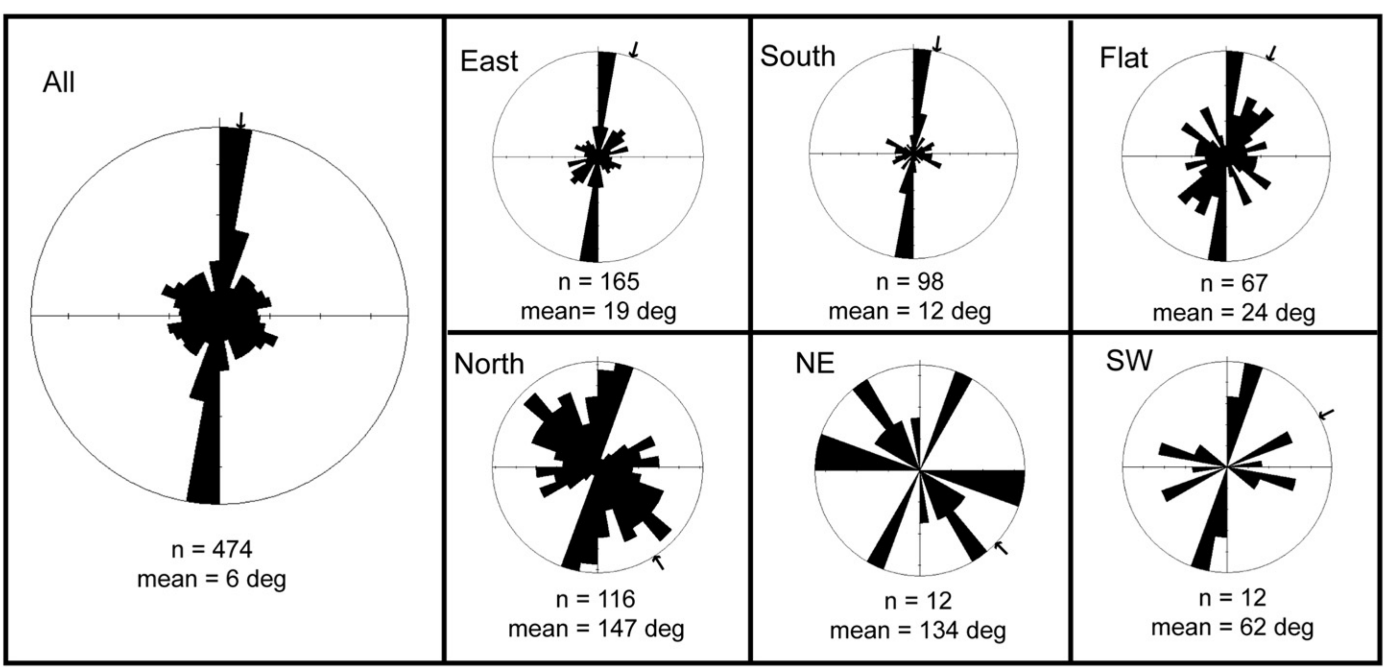


**Fig. 6.** Crack orientation for all data, as well as for subsets of this dataset separated according to slope direction. Total data includes four measurements on west-facing slopes not illustrated as an independent rose diagram. Arrows indicate vector mean values in degrees, which are also listed as "mean" for each diagram. Tick marks on axes indicate 5% for all rose diagrams.

**Table 6**
Orientation data for both vertical cracks and pavement clasts, including number counted ($n$), vector mean (mean) in degrees, circular standard deviation, circular skewness, circular kurtosis, circular variance and von Mises–Fisher distribution kappa values.

Crack orientations

| Slope aspect | $n$ | Mean | Variance | Stdev | Skewness | Kurtosis | Kappa |
|---|---|---|---|---|---|---|---|
| All | 474 | 6 | 0.85 | 2.0 | 0.05 | 0.23 | 0.30 |
| East | 165 | 19 | 0.76 | 1.7 | −0.14 | 0.22 | 0.49 |
| North | 116 | 147 | 0.78 | 1.7 | 0.10 | −0.05 | 0.45 |
| South | 98 | 12 | 0.76 | 1.7 | −0.13 | 0.69 | 0.49 |
| Flat | 67 | 24 | 0.83 | 1.9 | −0.01 | 0.21 | 0.35 |
| NE | 12 | 134 | 0.63 | 1.4 | −0.38 | −0.01 | 0.80 |
| SW | 12 | 62 | 0.90 | 2.1 | 0.29 | −0.59 | 0.21 |
| West | 4 | 109 | 0.58 | 1.3 | 0.05 | −1.70 | 0.93 |

Pavement orientations

| Site name | $n$ | Mean | Variance | Stdev | Skewness | Kurtosis | Kappa | Slope index |
|---|---|---|---|---|---|---|---|---|
| 07PV13 | 485 | 36 | 0.87 | 2.0 | −0.05 | 0.06 | 0.27 | 0 |
| 07PV25 | 576 | 13 | 0.87 | 2.0 | −0.05 | 0.13 | 0.26 | 0 |
| 07PV33 | 102 | 2 | 0.91 | 2.2 | −0.19 | −0.04 | 0.18 | 0 |
| A2000 | 289 | 11 | 0.91 | 2.2 | −0.07 | 0.04 | 0.18 | 0 |
| S1051 | 303 | 162 | 0.94 | 2.4 | −0.04 | 0.01 | 0.12 | 0 |
| S1102 | 463 | 13 | 0.85 | 2.0 | 0.07 | 0.00 | 0.30 | 0 |
| 07PV01 | 138 | 4 | 0.87 | 2.0 | 0.07 | 0.22 | 0.26 | 0 |
| PAV011 | 451 | 19 | 0.97 | 2.6 | −0.07 | −0.07 | 0.06 | 0 |
| 07PV05 | 321 | 19 | 0.88 | 2.1 | −0.04 | −0.04 | 0.24 | 1 |
| 07PV08 | 295 | 52 | 0.92 | 2.3 | 0.00 | −0.01 | 0.15 | 1 |
| 07PV17 | 277 | 16 | 0.94 | 2.4 | 0.01 | −0.1 | 0.11 | 1 |
| S2100 | 438 | 76 | 0.95 | 2.4 | 0.05 | −0.01 | 0.10 | 1 |
| S3062 | 160 | 45 | 0.97 | 2.7 | −0.12 | 0.05 | 0.06 | 1 |
| S4118 | 404 | 34 | 0.96 | 2.6 | −0.07 | −0.03 | 0.07 | 1 |
| PAV013 | 469 | 11 | 0.93 | 2.3 | −0.02 | 0.02 | 0.13 | 2 |
| S2012 | 492 | 30 | 0.90 | 2.2 | −0.10 | −0.09 | 0.19 | 2 |
| 07PV49 | 548 | 156 | 0.95 | 2.5 | 0.08 | −0.11 | 0.09 | 2 |
| S4012 | 322 | 135 | 0.85 | 2.0 | 0.03 | 0.04 | 0.30 | 2 |
| S4017 | 418 | 14 | 0.96 | 2.5 | −0.03 | 0.02 | 0.09 | 2 |
| S4041 | 259 | 38 | 0.86 | 2.0 | −0.14 | 0.02 | 0.29 | 2 |
| S4077 | 659 | 40 | 0.90 | 2.1 | 0.00 | −0.01 | 0.21 | 2 |
| 07PV35 | 375 | 43 | 0.94 | 2.3 | −0.03 | −0.07 | 0.13 | 3 |
| 07PV45 | 315 | 11 | 0.91 | 2.2 | 0.03 | 0.02 | 0.18 | 3 |
| S1032 | 485 | 32 | 0.85 | 2.0 | 0.04 | −0.03 | 0.30 | 3 |
| S2023 | 457 | 42 | 0.85 | 1.9 | 0.00 | 0.02 | 0.30 | 3 |
| S3127 | 301 | 5 | 0.90 | 2.2 | −0.03 | 0.15 | 0.19 | 3 |
| S4003 | 381 | 44 | 0.93 | 2.3 | 0.10 | −0.03 | 0.14 | 3 |

clasts with random orientations (Fig. 7). All $\kappa$ values are greater than zero, indicating some level of orientation, but $\kappa$ values vary from 0.09 to 0.39 and only three pavements provide $\kappa$ values $\geq$0.3, exhibiting the highest level of orientation in this dataset. Examination of these orientations grouped according to slope indices (Fig. 7, Table 6), in addition to Spearman rank order correlation of slope indices with pavement $\kappa$ values (Table 3), indicates no relationship between increasing slope and increased orientation as measured by $\kappa$ values; the variation shown here cannot be directly explained by any particular feature of the local landscape or of the pavements themselves.

The lack of correlation between $\kappa$ values and slope suggests that slope-controlled processes such as overland flow and gravity-driven creep have not been the controlling factors in clast orientation. In fact the largest $\kappa$ values determined for pavement orientations can be found on both flat and steep slopes (Table 6). Lateral transport of pavement clasts has probably been minimal during pavement development, as transport of clasts on slopes would presumably have led to preferred clast orientations (e.g., Anderson et al., 2002). Similarly, the lack of a meridional preferred orientation in pavements indicates that the northerly wind in this region is not causing a preferred clast orientation, and that thermally-controlled shattering is not the only process acting upon pavements at the surface. We would expect shattering alone to result in pavements with similar orientations to those measured for vertical cracks (Fig. 6) and for this orientation to be more significantly correlated with pavements containing more chert cobbles, which are the clasts being affected by thermal stresses. Instead, we see no correlation between chert content and $\kappa$ values (Table 4). Kappa values measured for pavement surfaces also show no spatial autocorrelation (Table 5, $Z > -1.96$), indicating random degrees of pavement orientation across our study area.

The bias involved in the determination of pavement orientation via photographic evidence leads to the preferential measurement of larger clasts. The movement and preferred orientation of clasts may be occurring at a scale smaller than that measured for pavement orientations here (e.g., movement of clasts <1–2 cm), as movement of smaller clasts would not be identified using this method. Orientation of larger clasts may have been inherited from fabrics present within gravel deposits or bedrock structure, or they may have been produced entirely through shrinking and swelling of underlying clays during pedogenesis, but any transport and orientation occurring at small scales would be invisible to the current study.

### 3.4. Desert soils

The soils found beneath the desert pavements on the Libyan Plateau almost always consist of a vesicular Av horizon varying in thickness (often between 3 and 7 cm thick) and consolidation (Fig. 5G) overlying a clast-free horizon of fine to coarse silts, and occasionally fine sands, of equally variable thickness. This clast-free layer in turn overlies the bedrock unit present in the area, which can be well-consolidated limestone bedrock, heavily weathered (silty) limestone, or chert-dominated gravel (Fig. 8). The silty horizon (B horizon) beneath the Av often reddens with proximity to limestone bedrock and sometimes

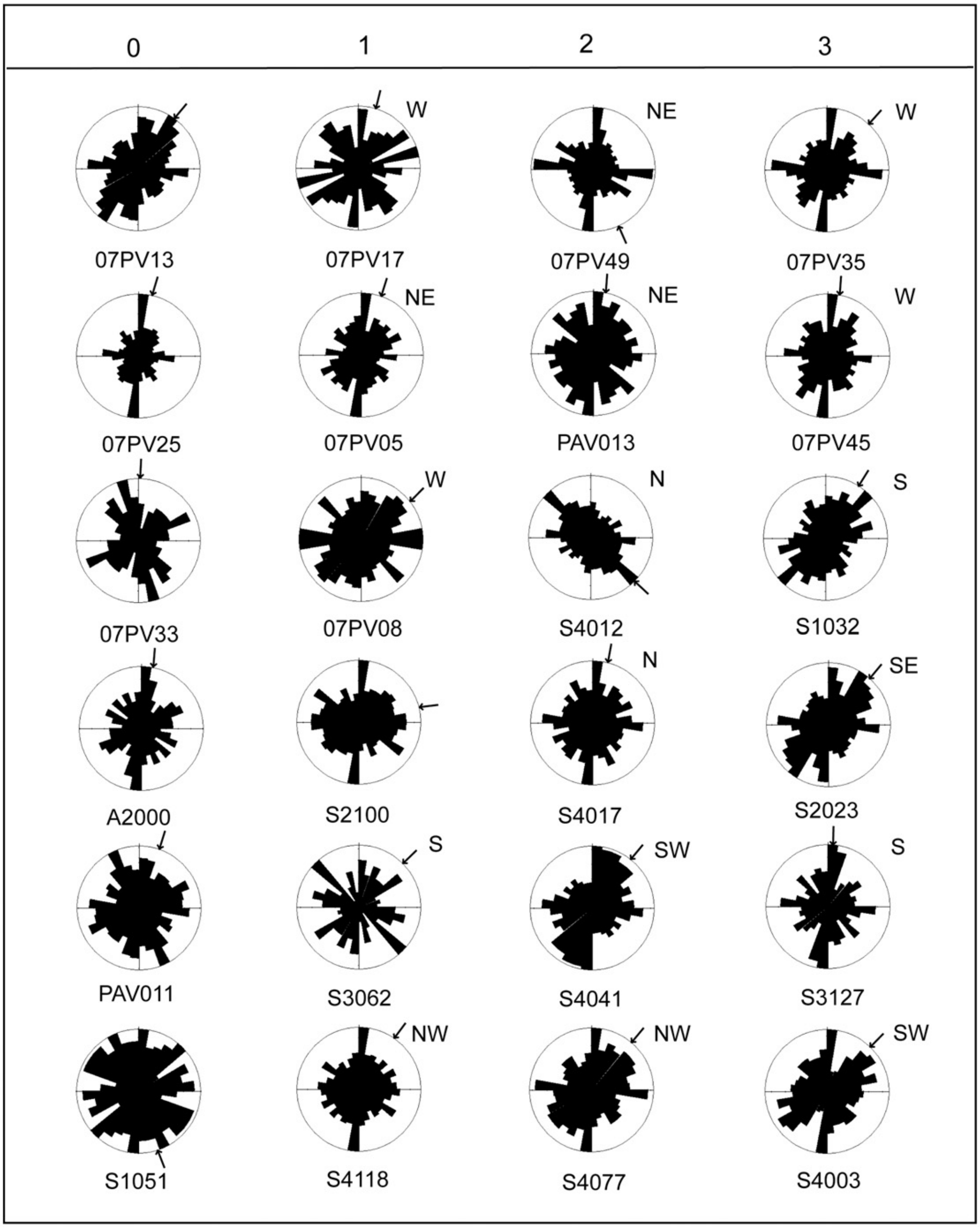


**Fig. 7.** Clast orientations for individual 0.25 m$^2$ sample areas determined by vectorizing observed clast orientations in ArcGIS 9.2 grouped according to slope gradient (0 = flat, 1 = gradual, 2 = moderate and 3 = steep). Arrows indicate vector mean values (see Table 6). Observed slope direction (where available) is indicated by directional symbols written at the top right-hand corner of each diagram. Tick marks on axes indicate 2% for all rose diagrams.

contains salts. Subsurface investigations revealed relatively clast-free horizons beneath all pavement surfaces. These clast-free horizons probably develop through the accumulation of aeolian materials beneath the pavement surface (McFadden et al., 1986, 1987). Pavements are limited in thickness to the overlap of only two clasts, where smaller clasts often occur beneath the edges of larger clasts. Where they are found in the subsurface, gravel clasts are small (often ≤1 cm in maximum diameter) and are found within the first 5 cm of the soil profile, often incorporated into particularly well-developed Av horizons (Fig. 5G). No visual evidence of desiccation cracking (slickensides, sediment infilling, modern cracks) is present in soil profiles.

Although development on flat surfaces as well as the presence of more easily weathered limestone bedrock (often found as more friable silty units) seem to lead to an increased depth of soil formation in many cases, there is no lack of thick soil horizons on gravel bedrock surfaces as well as on steeper slopes (Fig. 8). Depth to bedrock can be 25 cm on the steepest slopes, whereas 39 cm to bedrock is the maximum measured depth in this study. In addition, qualitative indices of Av development (1 = poor, 2 = moderate, 3 = well-developed) are not strongly correlated with Av horizon thickness (corrected Spearman rank correlation 0.17, $t = 1.20$, $n = 50$) or depth to bedrock (corrected Spearman rank correlation = −0.12, $t = -0.79$, $n = 48$). Similarly, Av horizon thickness is not related to the depth of the soil column as a whole or to the population density, burial, or size of pavement clasts ($r^2 = 0$ for all linear regressions), suggesting that Av development (qualitative determination of vesicularity and consolidation, measurement of horizon thickness) is not an indication of soil development but is more likely related to specific shrink-swell

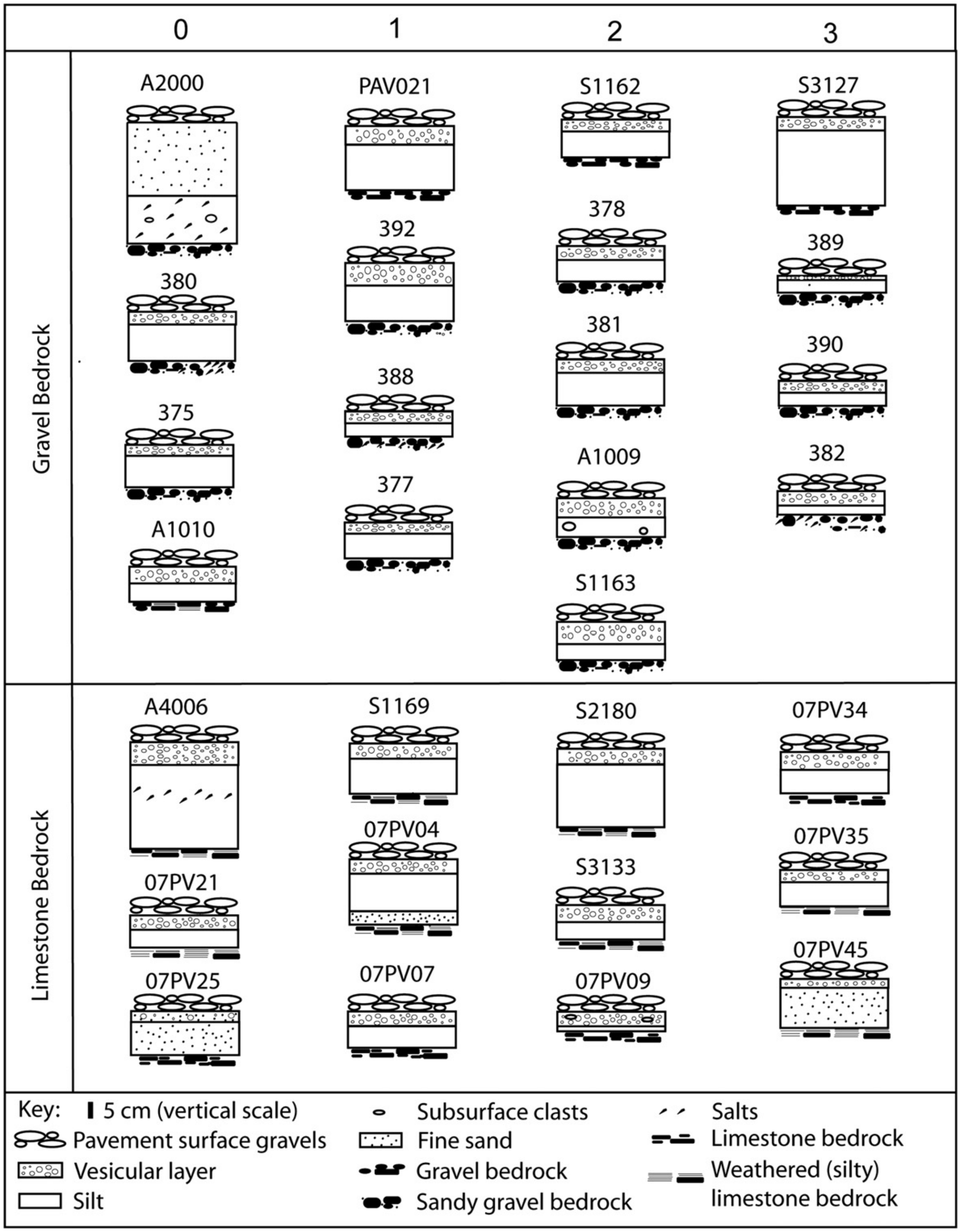


**Fig. 8.** Example soil profiles from the ASPS study area illustrated according to observed slope index (0 = flat, 3 = steep) and bedrock composition (gravels versus limestones).

and permeability conditions at the surface of any given pavement sample. However, the fact that Av development indices are not directly related to either clast density (corrected Spearman rank correlation = −0.16, $t = -1.11$, $n = 50$) or burial (corrected Spearman rank correlation = −0.15, $t = -1.02$, $n = 50$) in turn suggests that the pavements themselves are not controlling soil formation or Av development.

The lack of discernable transport of clasts (e.g., lack of clast orientation or correlation between clast size and slope gradient) on desert pavement surfaces and the relative stability of this landscape indicated by the development of accretionary pavement surfaces suggest that erosion has not been significant on the Libyan Plateau during the Quaternary. The thickness of desert soils, particularly the clast-free B horizons of these soils, on many steep slopes and the lack of any direct relationship between slope and the depth of soil formation indicate that slope probably has no direct effect on the thickness of soil horizons, and that the ability of gravel surfaces to trap aeolian dust played the largest role in increasing the thickness of these soils. The extent to which a given surface would act as an effective dust trap may be controlled by a variety of factors including wind velocity and gravel roughness during any given time period (Dong et al., 2002), as well as the amount of vegetation present (Gerson and Amit, 1987). However, the variable importance of these particular controls on dust accumulation would not be discernable from the soil characteristics examined here.

## 4. Discussion

The clast measurements made here fail to delineate any subset of pavement surfaces containing lower than average clast sizes or higher coverage by smaller clasts compared to those in other areas. This suggests that, unlike desert fan surfaces (e.g., Al-Farraj and Harvey, 2000), there are either no significant differences in the ages of desert pavement surfaces found on the eastern Libyan Plateau, or all surfaces are old enough to have evolved to an equilibrium form where clast parameters can no longer be used to distinguish between pavements of different age. The area examined in this study exhibits seemingly random and gradual change in almost all pavement characteristics including clast coverage, with only slightly significant clustering in clast size. The lack of distinct surfaces of different identifiable ages allows us to use the entire Plateau pavement as a single entity, where any differences between pavement samples are more likely the result of localized landscape changes, *in situ* soil formation processes such as shrink/swell of Av horizon clays, or pre-existing bedrock conditions instead of maturity differences between soils on the Plateau.

The data obtained from desert pavement surfaces across this study area indicate very few spatial patterns in pavement characteristics. The seemingly random variation in pavement parameters other than clast size and lithology suggests that the development of the modern desert pavements has not been controlled by any specific external surface process, and is more likely the result of the variable nature of the preexisting bedrock and gravel units from which these pavements are derived. The degree of clast orientation is not related to slope gradient and is not spatially autocorrelated, suggesting that pavement clasts, as well as any associated archaeological materials, would not have been affected by significant overland flow or other gravity-driven processes that would orient surface clasts. Clast size also has no relationship to slope gradient, suggesting that slopes have not had a significant impact of clast sorting. The accretionary nature of the soils on the Plateau additionally suggest limited erosion or transport of surface sediments in this region, and a number of identifiable *in situ* weathering processes provide a mechanism for desert pavement formation without lateral transport. The lack of developmental control by any measured geomorphic parameter, particularly slope, indicates a very stable landscape on the eastern Libyan Plateau.

Lowering of this landscape has probably been punctuated and slow, with erosion affecting only the outermost edges of the plateau and wadi heads as slopes have retreated over time. The stability of the plateau appears to be lateral in nature, both because erosion is moving inward from the plateau edges and because soil formation mechanisms may still be acting vertically upon each pavement surface on a small (site-relevant) scale. Pavement surfaces would therefore be extremely stable in a lateral sense, whereas the associated desert soils would exhibit much more significant vertical change over time. Downward migration of surface clasts can occur through repeated trampling, although vertical movement is limited in fine-grained contexts, such as those on the Libyan Plateau, compared to sandy sediments (Gifford-Gonzalez et al., 1985). However, vertical displacement can occur on the scale of centimeters, particularly through the upward mixing of particles by biogenic activity (Moeyersons, 1978) or through the closure of desiccation cracks (Moeyersons et al., 2006). Mixing of materials vertically may be considerably more significant than lateral displacement within or between stratigraphic units (Villa, 1982), such as the soil horizons examined here.

On gravel surfaces, particularly those underlain by well-consolidated units, surface runoff results in only minimal creep (several mm of movement) downslope, or upslope in the case of whirlpool formation on the upslope side of pebbles (de Ploey and Moeyersons, 1975). Even the smallest clasts present within the pavement surface are therefore moving laterally only on the scale of millimeters, if at all, during rainfall events. The primary processes acting upon pavements seem to be the accumulation of dust and thickening of an accretionary layer, as evidenced by the ubiquitous presence of a clast-free silt layer beneath pavement surfaces, which is present regardless of the underlying bedrock composition. The continual accretion of this silt serves to buoy coarser clasts at the surface as finer sediments are washed beneath (Wells et al., 1985; McFadden et al., 1986, 1987; Wells et al., 1995).

Coarse gravels can serve as an efficient dust trap due to their high porosity, permeability and surface roughness (Gerson and Amit, 1987), particularly when gravel coverage exceeds 15% (Dong et al., 2002), as it does throughout this study area. Rates of dust entrapment may have varied significantly over even short periods of geologic time, just as dust fluxes in the Western US have been shown to be significantly variable during the Quaternary (e.g., McFadden et al., 1987; Reheis and Kihl, 1995). Climate fluctuations may lead to variations in aeolian entrapment due to variations in the deposition of atmospheric dust and the availability of dust for transport as well as changes in local controls on dust preservation, such as the presence of vegetation (e.g., Gerson and Amit, 1987; Prospero and Lamb, 2003; Pelletier, 2007). It is also likely that during the early stages of pavement formation these surfaces accumulated dust at a faster rate than at present, due to their more open surfaces (lower clast coverage) and their increased aerodynamic roughness (which decreases through weathering over time) (Gerson and Amit, 1987).

An increase in dust availability would, in turn, increase the rate of accretionary layer formation. During periods of increased dust accumulation small clasts may have been buried by the accumulating accretionary layer even as the larger pavement clasts remained at the surface, or these smaller clasts may have worked their way down into underlying soil horizons through other pedogenic processes including bioturbation and shrink/swell process. Small clasts are found within the Av horizon in many cases (Figs. 5G, 8). Given the lack of evidence for lateral transport of clasts, the primary concern for archaeologists from a taphonomic standpoint should be pedogenic processes and the loss of smaller clasts on a very small lateral scale as well as vertical movement within the first few centimeters of the Av horizon.

The primary difficulty in examining data at the small scales relevant to the taphonomy of individual artifacts and artifact assemblages is that the conditions present at a given pavement surface are not necessarily similar to those of the larger landscape, whereas the majority of the (DEM-derived) data available concerning regional geomorphology utilizes a much larger scale of inquiry. However, even a semi-quantitative examination of the major potential geomorphic controls, specifically slope-related effects, on pavement formation indicates that the relationship between hillslope processes (e.g., overland flow, gravity-driven creep) and pavement development is not strong. This, in turn, suggests that pavement development has been controlled *in situ* with primary alteration through vertical processes. The archaeological materials preserved in this region have probably been preserved with their horizontal position intact, similar to surface artifact scatters in Australia (Fanning and Holdaway, 2001).

The majority of surface studies in arid environments reveal spatial patterns in the distribution of clast burial, lithology and orientation, and often invoke surface runoff and gravity-driven, slope-controlled clast transport as local controls on these spatial variations (e.g., Frostick and Reed, 1983; Abrahams et al., 1990; Poesen et al., 1998). The lack of similar spatial relationships on the Libyan Plateau suggests a lack of runoff- or gradient-controlled pavement development in this region, which in turn indicates a lack of significant erosion or slope movement during pavement formation. The stability of these pavement surfaces is supported by the presence of thick Av horizons, which may take several thousands of years to develop (e.g., Anderson et al., 2002).

## 5. Conclusions

Desert pavements examined on the eastern Libyan Plateau adjacent to the Nile Valley near Abydos, Egypt, do not exhibit areas of identifiably variable maturation that would indicate different ages for pavement surfaces. Clast size, density, lithology, and orientation within pavements have not been directly influenced by slope gradient or aspect, indicating that bedrock was the most likely primary control on pavement lithology but also that pavement formation has been largely undisturbed by local surface processes including overland flow and slope retreat. A preferential N–S orientation in vertical cracks in surface clasts in this study area indicates thermal control on some mechanical breakdown of chert clasts on the surface, which contributes to the overall development of pavements by creating smaller clasts and larger clast populations over time. Mechanical weathering may have been aided by salts, which are present in many soil profiles, as well as freeze-thaw and hydration shattering processes. However, a lack of preferred orientation for clasts within most pavements indicates that solar fracture was not a significant control on resulting clast orientations, nor was lateral clast transport a primary mechanism in pavement development on slopes. The lack of orientation of clasts within pavements is consistent with desert pavements as a product of the bedrock and sediment present prior to pavement development, and suggests that slope retreat, surface runoff and gravity-driven clast movements have had very little effect on pavement clasts or pavement formation.

The lack of influence of external controls suggests that pavement development in this area has been a function of *in situ* desert soil formation mechanisms, including shrink/swell within a vesicular accretionary Av horizon and the maintenance of a gravel pavement surface through the accumulation and down-washing of fine sediments. The presence of refitting Middle and Upper Paleolithic artifacts on these pavement surfaces (Chiotti et al., 2007) in addition to the apparent *in situ* control of pavement characteristics indicate a minimum of approximately one hundred thousand years of stability in this area, even if the pavements themselves have not been actively developing throughout this period. Archaeological materials found in surface contexts in this region have therefore been preserved with minimal, small-scale taphonomic effects wherever pavement surfaces are found intact.

## Acknowledgements

We are indebted to the Abydos Survey for Paleolithic Sites, particularly to Harold Dibble, Shannon McPherron, Deborah Olszewski, Isabelle Couchoud, Utsav Schurmans, and Laurent Chiotti. Funding for ASPS was provided by the University of Pennsylvania Museum of Archaeology and Anthropology, the Leakey Foundation, and National Science Foundation Grant 544928. Support was also provided by the Max Planck Institute for Evolutionary Anthropology (Leipzig, Germany). This research was additionally funded by a National Science Foundation Graduate Research Fellowship (to KAA). We would like to thank the Egyptian Supreme Council for Antiquities, Secretary General Zahi Hawass, and the Penn-Yale-IFA Expedition for permissions to do this work, as well as the crew, guards and inspectors associated with ASPS for their help, protection and survey efforts in the field. We would also like to thank two anonymous reviewers for their thoughtful comments on the initial version of this manuscript. This is ASPS Contribution No. 7.

## Appendix A

All data used for pavement comparisons: UTM coordinates (easting and northing), surface area calculated for all chert clasts ($cm^2$), % chert clasts in sample, number of chert clasts in sample, burial value for sample, density value for sample, average surface area of all clasts in sample ($cm^2$), median surface area for the sample ($cm^2$), standard deviation of surface areas for the sample ($cm^2$). Slope (°), aspect (°), and elevation (m) of sample localities obtained from ASTER DEM. Slope index values indicate relative gradient, where 0 = flat, 1 = gradual, 2 = moderate and 3 = steep.

| Site | Easting | Northing | Chert area[a] | % Chert | # Chert | Burial[b] | Density[c] | Av. area | Median | Stdev | Slope (DEM) | Slope (index) | Aspect | Elevation |
|---|---|---|---|---|---|---|---|---|---|---|---|---|---|---|
| A1009 | 389519 | 2887298 | 411.90 | 91.53 | 115 | 2.25 | 0.69 | 3.28 | 1.53 | 6.90 | 1.72 | 2 | 33.69 | 293 |
| A2000 | 388751 | 2885866 | 855.78 | 96.64 | 125 | 4.43 | 0.69 | 6.46 | 1.53 | 33.87 | 3.18 | 0 | 257.01 | 261 |
| A3005 | 389309 | 2885552 | 397.62 | 92.48 | 82 | 2.15 | 0.60 | 3.61 | 1.53 | 8.92 | 4.76 | 0 | 90.00 | 249 |
| A4005 | 388764 | 2885469 | 198.30 | 45.59 | 21 | 1.45 | 0.38 | 3.82 | 0.75 | 10.20 | 5.81 | 0 | 145.01 | 211 |
| A4006 | 388764 | 2885486 | 341.84 | 63.92 | 42 | 1.78 | 0.41 | 4.31 | 1.68 | 7.31 | 6.67 | 0 | 175.91 | 214 |
| PAV001 | 388947 | 2885815 | 276.19 | 96.53 | 117 | 1.43 | 0.63 | 2.27 | 1.16 | 3.67 | 5.24 | 1 | 90.00 | 263 |
| PAV002 | 388567 | 2885772 | 415.31 | 91.44 | 140 | 2.27 | 0.77 | 2.97 | 1.53 | 3.00 | 3.52 | 2 | 298.30 | 253 |
| PAV003 | 388731 | 2885717 | 603.23 | 98.41 | 122 | 3.06 | 0.72 | 4.26 | 1.53 | 14.72 | 9.72 | 3 | 198.43 | 250 |
| PAV004 | 388391 | 2885564 | 378.74 | 88.30 | 112 | 2.14 | 0.69 | 3.13 | 1.53 | 4.53 | 6.80 | 2 | 102.09 | 259 |
| PAV005 | 388460 | 2885366 | 244.22 | 69.72 | 78 | 1.75 | 0.59 | 2.97 | 1.53 | 6.37 | 10.56 | 2 | 100.30 | 245 |
| PAV006 | 388492 | 2885047 | 41.84 | 9.66 | 5 | 2.16 | 0.68 | 3.18 | 0.75 | 10.30 | 13.07 | 0 | 338.96 | 226 |
| PAV007 | 388940 | 2885328 | 285.03 | 80.88 | 82 | 1.76 | 0.55 | 3.23 | 1.53 | 5.11 | 10.70 | 1 | 221.42 | 201 |
| PAV008 | 389125 | 2885491 | 156.63 | 23.27 | 32 | 2.24 | 0.36 | 6.17 | 2.99 | 9.41 | 6.26 | 0 | 188.75 | 244 |
| PAV009 | 389130 | 2885684 | 225.34 | 57.75 | 70 | 1.95 | 0.66 | 2.96 | 1.53 | 4.91 | 4.69 | 3 | 113.96 | 261 |
| PAV010 | 389786 | 2885753 | 276.36 | 79.01 | 100 | 1.75 | 0.77 | 2.29 | 1.53 | 3.16 | 6.99 | 2 | 9.78 | 208 |
| PAV011 | 389342 | 2885810 | 690.14 | 97.41 | 147 | 3.54 | 0.79 | 4.48 | 1.53 | 12.77 | 9.14 | 0 | 73.44 | 234 |
| PAV012 | 389444 | 2885712 | 221.94 | 57.95 | 46 | 1.91 | 0.93 | 2.07 | 0.75 | 5.22 | 11.04 | 2 | 70.02 | 219 |
| PAV013 | 389645 | 2885605 | 133.50 | 32.26 | 23 | 2.07 | 0.66 | 3.13 | 1.53 | 5.38 | 0.75 | 2 | 18.43 | 185 |
| PAV014 | 386292 | 2886551 | 389.29 | 88.66 | 133 | 2.20 | 0.95 | 2.32 | 0.68 | 9.77 | 7.75 | 0 | 229.97 | 277 |
| PAV015 | 386515 | 2886608 | 303.91 | 92.02 | 112 | 1.65 | 0.63 | 2.62 | 0.68 | 8.61 | 4.68 | 1 | 104.74 | 283 |
| PAV016 | 393565 | 2882787 | 192.69 | 78.44 | 85 | 0.82 | 0.39 | 2.08 | 1.53 | 2.53 | 0.34 | 0 | 225.00 | 162 |
| PAV017a | 385262 | 2885639 | 792.86 | 79.58 | 371 | 1.99 | 1.01 | 1.97 | 0.79 | 5.35 | 11.08 | 0 | 181.22 | 277 |
| PAV017b | 385262 | 2885639 | 112.31 | 74.00 | 65 | 1.52 | 1.04 | 1.46 | 0.79 | 1.36 | 11.08 | 0 | 181.22 | 277 |
| PAV017c | 385262 | 2885639 | 136.27 | 80.98 | 85 | 1.68 | 1.08 | 1.56 | 0.79 | 1.76 | 11.08 | 0 | 181.22 | 277 |
| PAV018a | 385090 | 2885609 | 359.12 | 99.46 | 124 | 1.81 | 0.64 | 2.84 | 1.18 | 5.98 | 7.97 | 1 | 239.62 | 264 |
| PAV018b | 385090 | 2885609 | 376.21 | 99.48 | 126 | 1.89 | 0.64 | 2.95 | 1.18 | 4.68 | 7.97 | 1 | 239.62 | 264 |
| PAV018c | 385090 | 2885609 | 266.25 | 95.83 | 141 | 1.39 | 0.79 | 1.76 | 0.79 | 3.79 | 7.97 | 1 | 239.62 | 264 |
| PAV019a | 385354 | 2885901 | 173.18 | 71.77 | 65 | 1.21 | 0.66 | 1.84 | 0.79 | 3.10 | 7.12 | 2 | 25.71 | 287 |
| PAV019b | 385354 | 2885901 | 225.02 | 69.75 | 92 | 1.61 | 0.85 | 1.92 | 1.18 | 2.18 | 7.12 | 2 | 25.71 | 287 |

(*continued on next page*)

**Appendix A** (*continued*)

| Site | Easting | Northing | Chert area[a] | % Chert | # Chert | Burial[b] | Density[c] | Av. area | Median | Stdev | Slope (DEM) | Slope (index) | Aspect | Elevation |
|---|---|---|---|---|---|---|---|---|---|---|---|---|---|---|
| PAV019c | 385354 | 2885901 | 266.25 | 76.65 | 88 | 1.74 | 0.75 | 2.32 | 1.18 | 5.06 | 7.12 | 2 | 25.71 | 287 |
| PAV020 | 388514 | 2886093 | 1045.65 | 87.05 | 436 | 2.00 | 0.87 | 2.30 | 1.96 | 2.41 | 10.07 | – | 309.29 | 255 |
| PAV021 | 386328 | 2883277 | 409.52 | 93.13 | 113 | 2.20 | 0.59 | 3.76 | 1.53 | 5.47 | 2.72 | 1 | 52.13 | 292 |
| S1004 | 389178 | 2885774 | 619.39 | 96.81 | 161 | 3.20 | 0.91 | 3.53 | 1.79 | 6.48 | 9.72 | 1 | 18.43 | 253 |
| S1030 | 389319 | 2885487 | 196.60 | 46.24 | 28 | 4.25 | 1.04 | 4.09 | 1.68 | 7.37 | 3.44 | 1 | 123.69 | 248 |
| S1032 | 389308 | 2885289 | 125.00 | 47.31 | 20 | 1.32 | 0.55 | 2.40 | 0.75 | 4.91 | 13.92 | 3 | 137.73 | 206 |
| S1040 | 386178 | 2888386 | 103.57 | 51.39 | 33 | 2.02 | 1.06 | 1.90 | 0.79 | 3.67 | 5.89 | 2 | 255.96 | 291 |
| S1051 | 385661 | 2888167 | 325.00 | 87.00 | 97 | 3.74 | 1.18 | 3.17 | 1.53 | 5.00 | 1.51 | 0 | 161.57 | 301 |
| S1095 | 384501 | 2886053 | 399.18 | 94.91 | 77 | 2.10 | 0.59 | 3.59 | 0.79 | 13.10 | 7.01 | 2 | 298.30 | 269 |
| S1102 | 384314 | 2885655 | 635.19 | 67.19 | 390 | 1.35 | 0.80 | 1.69 | 1.18 | 2.29 | 8.56 | 0 | 104.42 | 253 |
| S1162 | 389444 | 2888111 | 454.08 | 88.10 | 159 | 2.58 | 1.00 | 2.58 | 1.53 | 3.69 | 12.11 | 2 | 60.95 | 297 |
| S1163 | 389587 | 2887796 | 249.83 | 85.47 | 76 | 2.92 | 1.08 | 2.71 | 1.53 | 3.98 | 6.18 | 2 | 157.38 | 265 |
| S1169 | 386527 | 2883288 | 665.14 | 98.05 | 95 | 2.26 | 0.37 | 6.17 | 1.53 | 18.20 | 3.44 | 1 | 326.31 | 289 |
| S2001 | 388728 | 2885876 | 335.88 | 93.41 | 117 | 1.80 | 0.67 | 2.68 | 1.53 | 4.17 | 3.39 | 1 | 230.71 | 260 |
| S2012 | 388260 | 2885762 | 273.30 | 90.16 | 143 | 1.52 | 0.85 | 1.78 | 1.53 | 1.86 | 5.95 | 2 | 267.71 | 258 |
| S2014 | 388729 | 2885711 | 412.93 | 99.48 | 141 | 2.08 | 0.72 | 2.88 | 1.53 | 3.90 | 8.53 | 1 | 180.00 | 249 |
| S2023 | 388872 | 2885041 | 0.00 | 0.00 | 0 | 1.41 | 0.71 | 1.99 | 0.75 | 5.08 | 11.20 | 3 | 81.53 | 230 |
| S2030 | 388104 | 2885033 | 288.95 | 81.65 | 105 | 1.77 | 0.73 | 2.42 | 1.53 | 2.69 | 5.44 | 2 | 23.20 | 237 |
| S2042 | 386029 | 2887995 | 400.34 | 90.75 | 77 | 2.21 | 0.56 | 3.94 | 0.79 | 10.94 | 12.66 | 0 | 139.51 | 293 |
| S2046 | 386222 | 2887840 | 267.86 | 75.80 | 67 | 1.77 | 0.61 | 2.90 | 1.53 | 4.77 | 2.13 | 0 | 333.43 | 275 |
| S2052 | 385670 | 2887715 | 211.56 | 70.77 | 79 | 1.49 | 0.74 | 2.03 | 0.79 | 3.02 | 7.42 | 2 | 140.19 | 296 |
| S2100 | 384890 | 2885729 | 239.94 | 87.04 | 96 | 1.38 | 0.63 | 2.21 | 1.18 | 3.99 | 4.39 | 1 | 167.47 | 264 |
| S2180 | 386676 | 2883021 | 312.59 | 94.74 | 111 | 1.10 | 0.42 | 2.62 | 1.53 | 3.94 | 1.35 | 2 | 315.00 | 287 |
| S3023 | 386558 | 2888158 | 75.17 | 37.62 | 31 | 2.00 | 1.09 | 1.83 | 0.79 | 2.79 | 1.72 | 2 | 56.31 | 270 |
| S3037 | 385316 | 2887343 | 284.86 | 84.41 | 100 | 1.69 | 0.74 | 2.30 | 1.53 | 4.46 | 5.48 | 1 | 235.62 | 297 |
| S3062 | 384521 | 2885930 | 458.28 | 95.11 | 79 | 2.41 | 0.52 | 4.68 | 1.18 | 8.36 | 5.75 | 1 | 204.44 | 266 |
| S3127 | 389677 | 2888868 | 495.92 | 93.56 | 103 | 2.65 | 0.69 | 3.84 | 1.53 | 9.36 | 2.05 | 3 | 324.46 | 290 |
| S3133 | 389611 | 2887439 | 362.07 | 93.73 | 93 | 1.93 | 0.55 | 3.51 | 1.53 | 6.54 | 9.75 | 2 | 345.96 | 282 |
| S4001 | 388725 | 2886176 | 305.61 | 75.34 | 80 | 1.35 | 0.40 | 3.35 | 1.79 | 5.02 | 3.02 | 3 | 341.57 | 268 |
| S4003 | 388888 | 2886059 | 412.59 | 87.37 | 102 | 2.36 | 0.71 | 3.33 | 1.53 | 7.04 | 2.90 | 3 | 350.54 | 268 |
| S4006 | 389172 | 2886025 | 177.72 | 88.14 | 83 | 2.02 | 1.04 | 1.94 | 1.53 | 2.66 | 11.49 | 2 | 28.14 | 257 |
| S4012 | 389393 | 2886152 | 82.99 | 18.24 | 21 | 4.55 | 1.12 | 4.06 | 1.14 | 7.99 | 14.76 | 2 | 18.43 | 202 |
| S4017 | 388960 | 2886282 | 552.21 | 96.03 | 106 | 2.88 | 0.65 | 4.42 | 1.53 | 7.62 | 15.64 | 2 | 53.47 | 233 |
| S4041 | 388161 | 2885397 | 351.53 | 98.11 | 164 | 3.58 | 1.70 | 2.11 | 0.68 | 5.51 | 4.86 | 2 | 191.31 | 269 |
| S4050 | 387908 | 2885320 | 387.76 | 77.49 | 88 | 2.50 | 0.69 | 3.63 | 1.53 | 6.90 | 3.84 | 2 | 119.74 | 273 |
| S4054 | 386512 | 2888439 | 220.58 | 73.53 | 78 | 1.50 | 0.68 | 2.21 | 0.79 | 4.54 | 5.43 | 0 | 52.13 | 270 |
| S4077 | 385276 | 2887703 | 206.80 | 93.67 | 84 | 1.10 | 0.57 | 1.94 | 0.79 | 2.85 | 4.68 | 2 | 284.74 | 304 |
| S4105 | 386027 | 2886429 | 448.98 | 91.61 | 108 | 2.45 | 0.64 | 3.83 | 2.25 | 4.91 | 10.65 | 0 | 102.80 | 300 |
| S4109 | 385984 | 2886891 | 307.31 | 81.23 | 101 | 1.89 | 0.73 | 2.61 | 1.53 | 3.57 | 8.10 | 1 | 290.56 | 295 |
| S4112 | 386147 | 2887011 | 302.04 | 68.74 | 92 | 2.20 | 0.84 | 2.62 | 1.53 | 3.15 | 8.79 | 2 | 297.26 | 292 |
| S4118 | 386480 | 2886435 | 346.09 | 88.30 | 96 | 1.96 | 0.62 | 3.19 | 1.53 | 4.74 | 5.01 | 1 | 182.73 | 268 |
| S4120 | 386795 | 2886480 | 167.86 | 81.35 | 70 | 2.06 | 1.08 | 1.91 | 1.53 | 1.89 | 3.20 | 2 | 63.43 | 267 |
| 07PV01 | 368050 | 2879026 | 127.89 | 90.92 | 92 | 0.47 | 0.36 | 1.30 | 0.68 | 1.77 | 5.81 | 0 | 124.99 | 308 |
| 07PV04 | 376264 | 2885366 | 329.59 | 99.77 | 124 | 1.10 | 0.42 | 2.64 | 1.53 | 2.51 | 3.52 | 1 | 28.30 | 294 |
| 07PV05 | 376123 | 2885556 | 268.03 | 87.41 | 117 | 1.02 | 0.45 | 2.29 | 1.53 | 2.68 | 0.75 | 1 | 71.57 | 292 |
| 07PV06 | 376078 | 2886088 | 234.69 | 88.18 | 81 | 1.33 | 0.57 | 2.36 | 0.75 | 3.20 | 3.39 | 2 | 309.29 | 292 |
| 07PV07 | 376307 | 2886342 | 144.39 | 58.15 | 62 | 0.83 | 0.44 | 1.90 | 1.53 | 3.18 | 3.11 | 1 | 274.40 | 294 |
| 07PV08 | 376415 | 2886768 | 251.19 | 91.82 | 82 | 1.37 | 0.54 | 2.53 | 1.53 | 5.53 | 3.02 | 1 | 108.43 | 284 |
| 07PV09 | 376358 | 2887460 | 200.17 | 67.27 | 50 | 1.49 | 0.61 | 2.46 | 0.75 | 6.27 | 6.42 | 2 | 357.88 | 269 |
| 07PV10 | 373329 | 2886885 | 128.40 | 82.80 | 76 | 0.78 | 0.52 | 1.51 | 0.68 | 2.50 | 1.01 | 0 | 45.00 | 291 |
| 07PV11 | 372075 | 2886868 | 94.39 | 81.76 | 134 | 0.58 | 0.90 | 0.64 | 0.19 | 1.06 | 1.43 | 1 | 90.00 | 301 |
| 07PV12 | 371438 | 2886899 | 38.10 | 80.01 | 71 | 0.48 | 1.02 | 0.47 | 0.19 | 0.59 | 2.36 | 1 | 135.00 | 299 |
| 07PV13 | 370970 | 2886900 | 39.46 | 77.03 | 77 | 0.51 | 1.00 | 0.51 | 0.19 | 0.58 | 2.64 | 0 | 275.19 | 298 |
| 07PV14 | 370339 | 2886977 | 146.77 | 59.57 | 63 | 0.82 | 0.37 | 2.20 | 0.75 | 6.28 | 0.95 | 1 | 90.00 | 301 |
| 07PV15 | 369082 | 2887022 | 195.24 | 78.83 | 57 | 0.62 | 0.28 | 2.23 | 0.75 | 3.78 | 1.72 | 1 | 56.31 | 292 |
| 07PV16 | 375261 | 2883112 | 161.56 | 77.96 | 69 | 0.69 | 0.36 | 1.94 | 1.53 | 1.96 | 1.35 | 1 | 135.00 | 309 |
| 07PV17 | 375362 | 2883591 | 237.07 | 85.94 | 83 | 0.69 | 0.29 | 2.40 | 1.53 | 3.33 | 1.01 | 1 | 315.00 | 304 |
| 07PV18 | 375294 | 2884574 | 105.10 | 65.56 | 36 | 0.80 | 0.67 | 1.21 | 0.75 | 1.84 | 0.95 | 1 | 90.00 | 291 |
| 07PV19 | 375645 | 2885094 | 289.12 | 94.45 | 85 | 1.02 | 0.37 | 2.73 | 1.53 | 3.24 | 2.86 | 2 | 90.00 | 289 |
| 07PV20 | 375248 | 2884894 | 383.33 | 100.00 | 112 | 1.28 | 0.37 | 3.42 | 1.53 | 4.22 | 1.69 | 1 | 261.87 | 294 |
| 07PV21 | 375223 | 2884202 | 177.55 | 81.64 | 55 | 0.72 | 0.39 | 1.84 | 0.75 | 2.90 | 3.44 | 0 | 303.69 | 301 |
| 07PV22 | 385923 | 2895191 | 0.00 | 0.00 | 5 | 1.20 | 0.27 | 4.50 | 1.68 | 15.00 | 8.70 | 0 | 150.64 | 281 |
| 07PV23 | 385609 | 2895182 | 4.25 | 3.28 | 1 | 1.30 | 1.28 | 1.02 | 0.75 | 1.46 | 5.96 | 1 | 298.61 | 298 |
| 07PV24 | 385485 | 2895200 | 7.65 | 5.38 | 2 | 0.71 | 0.82 | 0.87 | 0.19 | 1.66 | 2.26 | 0 | 18.43 | 288 |
| 07PV25 | 385101 | 2895520 | 12.59 | 13.87 | 4 | 0.45 | 0.62 | 0.73 | 0.75 | 0.92 | 2.46 | 0 | 60.95 | 315 |
| 07PV26 | 384920 | 2895594 | 100.51 | 37.84 | 33 | 1.33 | 0.54 | 2.48 | 1.53 | 3.14 | 2.46 | 1 | 150.95 | 310 |
| 07PV27 | 384915 | 2895219 | 277.55 | 82.89 | 55 | 1.12 | 0.36 | 3.07 | 0.75 | 6.01 | 6.06 | 2 | 244.44 | 305 |
| 07PV28 | 384878 | 2895679 | 3.57 | 5.04 | 4 | 0.71 | 1.24 | 0.57 | 0.43 | 0.50 | 0.68 | 1 | 135.00 | 312 |
| 07PV29 | 384672 | 2895738 | 23.81 | 20.76 | 4 | 1.15 | 1.13 | 1.01 | 0.75 | 1.68 | 3.39 | 0 | 309.29 | 303 |
| 07PV30 | 384672 | 2895738 | 2.72 | 2.78 | 1 | 0.98 | 1.05 | 0.93 | 0.19 | 1.49 | 3.39 | 0 | 309.29 | 303 |
| 07PV31 | 385019 | 2896013 | 56.80 | 23.06 | 19 | 0.82 | 0.45 | 1.84 | 0.75 | 2.48 | 1.22 | 1 | 348.69 | 302 |
| 07PV32 | 384867 | 2895201 | 40.48 | 21.44 | 8 | 0.94 | 0.67 | 1.41 | 0.75 | 2.90 | 2.02 | 0 | 225.00 | 302 |
| 07PV33 | 384239 | 2894745 | 210.71 | 54.65 | 32 | 0.77 | 0.23 | 3.35 | 0.75 | 4.72 | 6.06 | 0 | 334.44 | 308 |
| 07PV34 | 384090 | 2894704 | 0.83 | 0.29 | 24 | 1.45 | 0.66 | 2.19 | 0.75 | 3.59 | 3.37 | 3 | 315.00 | 297 |
| 07PV35 | 383710 | 2894477 | 290.99 | 90.43 | 105 | 1.61 | 0.65 | 2.49 | 1.53 | 3.49 | 2.57 | 3 | 338.20 | 285 |
| 07PV36 | 383573 | 2894333 | 69.56 | 46.18 | 33 | 1.51 | 1.03 | 1.46 | 0.79 | 1.70 | 5.23 | 3 | 149.93 | 292 |
| 07PV37 | 383460 | 2894403 | 494.73 | 91.83 | 97 | 1.80 | 0.38 | 4.68 | 2.72 | 6.94 | 3.18 | 0 | 102.99 | 303 |

**Appendix A** (*continued*)

| Site | Easting | Northing | Chert area[a] | % Chert | # Chert | Burial[b] | Density[c] | Av. area | Median | Stdev | Slope (DEM) | Slope (index) | Aspect | Elevation |
|---|---|---|---|---|---|---|---|---|---|---|---|---|---|---|
| 07PV38 | 388764 | 2893226 | 697.11 | 99.33 | 98 | 2.34 | 0.35 | 6.68 | 2.72 | 10.58 | 5.10 | 1 | 307.41 | 289 |
| 07PV39 | 388934 | 2893134 | 252.55 | 91.71 | 87 | 1.38 | 0.52 | 2.67 | 1.53 | 3.21 | 4.50 | 1 | 302.01 | 304 |
| 07PV40 | 389015 | 2893057 | 392.01 | 98.09 | 131 | 2.00 | 0.68 | 2.94 | 1.53 | 3.70 | 5.06 | 1 | 221.19 | 313 |
| 07PV41 | 390197 | 2893376 | 309.18 | 88.58 | 108 | 1.75 | 0.71 | 2.48 | 1.53 | 2.80 | 6.47 | 1 | 53.97 | 295 |
| 07PV42 | 389905 | 2893287 | 417.18 | 97.68 | 116 | 2.14 | 0.63 | 3.39 | 0.68 | 15.88 | 6.70 | 1 | 152.53 | 308 |
| 07PV43 | 389840 | 2893190 | 167.52 | 79.61 | 79 | 1.05 | 0.62 | 1.71 | 0.75 | 2.71 | 3.58 | 1 | 86.19 | 298 |
| 07PV44 | 389664 | 2893084 | 181.29 | 74.04 | 39 | 1.22 | 0.50 | 2.45 | 0.75 | 6.09 | 4.39 | 2 | 310.60 | 308 |
| 07PV45 | 389451 | 2893143 | 296.43 | 97.78 | 129 | 1.52 | 0.69 | 2.21 | 1.53 | 3.25 | 3.11 | 3 | 85.60 | 297 |
| 07PV46 | 388833 | 2895034 | 11.71 | 25.68 | 10 | 1.00 | 1.15 | 1.91 | 0.75 | 4.76 | 6.89 | 0 | 268.03 | 280 |
| 07PV47 | 388985 | 2895003 | 106.80 | 42.52 | 17 | 1.26 | 0.63 | 1.99 | 0.75 | 5.12 | 5.23 | 0 | 30.07 | 278 |
| 07PV48 | 389243 | 2894867 | 489.80 | 89.20 | 74 | 1.83 | 0.38 | 4.86 | 1.53 | 17.34 | 10.36 | 0 | 43.15 | 291 |
| 07PV49 | 389159 | 2895053 | 100.68 | 38.95 | 17 | 1.29 | 0.78 | 1.66 | 0.75 | 2.70 | 22.37 | 2 | 31.76 | 254 |

[a]Total surface area for all chert clasts counted. Individual clast surface areas calculated as (measured maximum length * (measured maximum length / (average length–width ratio for this lithology from Table 2))).
[b]Burial calculated as (Total calculated surface area of all clasts / total surface area of counted squares within the sample).
[c]Density calculated as (Total # clasts counted / total surface area of counted squares within the sample).

## References


Abrahams, A.D., Soltyka, N., Parsons, A.J., Hirsch, P.J., 1990. Fabric analysis of a desert debris slope: Bell Mountain, California. Journal of Geology 98, 264–272.

Al-Farraj, A., Harvey, A.M., 2000. Desert pavement characteristics on wadi terrace and alluvial fan surfaces: Wadi Al-Bih, U.A.E. and Oman. Geomorphology 35, 279–297.

Allison, R.J., Grove, J.R., Higgitt, D.L., Kirk, A.J., Rosser, N.J., Warburton, J., 2000. Geomorphology of the eastern Badia basalt plateau, Jordan. The Geographical Journal 166, 352–370.

Amit, R., Gerson, R., Yaalon, D.H., 1993. Stages and rate of the gravel shattering process by salts in desert Reg soils. Geoderma 57, 295–324.

Anderson, K., Wells, S., Graham, R., 2002. Pedogenesis of vesicular horizons, Cima Volcanic Field, Mojave Desert, California. Soil Science Society of America Journal 66, 878–887.

Briggs, D., 1977. Sources and Methods in Geography: Sediments. Butterworths, London. 192 pp.

Chiotti, L., Olszewski, D.I., Dibble, H.L., McPherron, S.R., Schurmans, U., Smith, J.R., 2007. Paleolithic Abydos: reconstructing individual behaviors across the high desert landscape. In: Hawass, Z., Richards, J. (Eds.), The Archaeology and Art of Ancient Egypt: essays in honor of David B. O'Connor. Supreme Council of Antiquities Press, Cairo, pp. 169–183.

Cockburn, H.A.P., Seidl, M.A., Summerfield, M.A., 1999. Quantifying denudation rates on inselbergs in the central Namib Desert using in situ-produced cosmogenic $^{10}$Be and $^{26}$Al. Geology 27, 399–402.

Cooke, R.U., 1970. Stone pavements in deserts. Annals of the Association of American Geographers 60, 560–577.

Cooke, R.U., Warren, A., 1973. Geomorphology in Deserts. University of California Press, Berkeley.

de Ploey, J., Moeyersons, J., 1975. Runoff creep of coarse debris: experimental data and some field observations. Catena 2, 275–288.

Dixon, J.C., 1994. Aridic soils, patterned ground, and desert pavements. In: Abrahams, A.D., Parsons, A.J. (Eds.), Geomorphology of Desert Environments. Chapman & Hall, London, pp. 64–81.

Dong, Z., Liu, Z., Wang, Z., 2002. Aerodynamic roughness of gravel surfaces. Geomorphology 43, 17–31.

Dorn, R.I., Oberlander, T.M., 1982. Rock varnish. Progress in Physical Geography 6, 317–367.

Fanning, P., Holdaway, S., 2001. Stone artifact scatters in western NSW, Australia: geomorphic controls on artifact size and distribution. Geoarchaeology: An International Journal 16, 667–686.

Fisher, N.I., Lewis, T., Embleton, B.J.J., 1987. Statistical Analysis of Spherical Data. Cambridge University Press, Cambridge. 329 pp.

Fisher, N.I., 1993. Statistical Analysis of Circular Data. Cambridge University Press, Cambridge. 277 pp.

Frostick, L., Reed, I., 1983. Taphonomic significance of sub-aerial transport of vertebrate fossils on steep semi-arid slopes. Lethaia 16, 157–164.

Gaven, C., Hillaire-Marcel, C., Petit-Maire, N., 1981. A Pleistocene lacustrine episode in southeastern Libya. Nature 290, 131–133.

Gerson, R., Amit, R., 1987. Rates and modes of dust accretion and deposition in an arid region — the Negev, Israel. In: Frostick, L., Reid, I. (Eds.), Desert Sediments: Ancient and Modern. Geological Society Special Publication No. 35, pp. 157–169.

Gifford-Gonzalez, D.P., Damrosch, D.B., Damrosch, D.R., Pryor, J., Thunen, R.L., 1985. The third dimension in site structure: an experiment in trampling and vertical dispersal. American Antiquity 50, 803–818.

Haff, P.K., Werner, B.T., 1996. Dynamical processes on desert pavements and the healing of surficial disturbances. Quaternary Research 45, 38–46.

Hoelzmann, P., Keding, B., Berke, H., Kröpelin, S., Kruse, H.-J., 2001. Environmental change and archaeology: lake evolution and human occupation in the Eastern Sahara during the Holocene. Palaeogeography, Palaeoclimatology, and Palaeoecology 169, 193–217.

Howard, A.D., 1967. Drainage analysis in geologic interpretation: a summation. American Association of Petroleum Geologists Bulletin 51, 2246–2259.

Klitzsch, E., List, F., Pohlmann, G., 1987. Geological Map of Egypt: NG 36 NW Asyut. Conoco-EGPC, Cairo.

Mardia, K.V., 1975. Statistics of directional data. Journal of the Royal Statistical Society. Series B (Methodological) 37, 349–393.

Mardia, K.V., Jupp, P.E., 1999. Directional Statistics. John Wiley & Sons, Ltd., New York. 429 pp.

McFadden, L.D., Wells, S.G., Dohrenwend, J.C., 1986. Influences of Quaternary climatic changes on processes of soil development on desert loess deposits of the Cima volcanic field, California. Catena 13, 361–389.

McFadden, L.D., Wells, S.G., Jercinovich, M.J., 1987. Influences of Eolian and Pedogenic processes on the origin and evolution of desert pavements. Geology 15, 504–508.

McFadden, L.D., Ritter, J.B., Wells, S.G., 1989. Use of multiparameter relative-age methods for age estimation and correlation of alluvial fan surfaces on a desert piedmont, eastern Mojave Desert, California. Quaternary Research 32, 276–290.

McFadden, L.D., McDonald, E.V., Wells, S.G., Anderson, K., Quade, J., Forman, S.L., 1998. The vesicular layer and carbonate collars of desert soils and pavements: formation, age and relation to climate change. Geomorphology 24, 101–145.

McFadden, L.D., Eppes, M.C., Gillespie, A.R., Hallet, B., 2005. Physical weathering in arid landscapes due to diurnal variation in the direction of solar heating. GSA Bulletin 117, 161–173.

McKenzie, J.A., 1993. Pluvial conditions in the eastern Sahara following the penultimate deglaciation: implications for changes in atmospheric circulation patterns with global warming. Palaeogeography, Palaeoclimatology, Palaeoecology 103, 95–105.

Miller, D.E., 1971. Formation of vesicular structure in soil. Proceedings - Soil Science Society of America 35, 635–637.

Mills, H.H., 1983. Clast-fabric strength in hillslope colluvium as a function of slope angle. Geografiska Annaler 65A, 255–262.

Moeyersons, J., 1978. The behaviour of stones and stone implements, buried in consolidating and creeping Kalahari sands. Earth Surface Processes and Landforms 3, 115–128.

Moeyersons, J., Nyssen, J., Poesen, J., Deckers, J., Haile, M., 2006. On the origin of rock fragment mulches on Vertisols: a case study from the Ethiopian highlands. Geomorphology 76, 411–429.

Moran, P.A.P., 1950. Notes on continuous stochastic phenomena. Biometrika 37, 17–23.

Nettleton, W.D., Peterson, F.F., 1983. Aridisols. In: Wilding, L.P., Smeck, N.E., Hall, G.F. (Eds.), Pedogenesis and Soil Taxonomy II. The Soil Orders. Developments in Soil Science IIB. Elsevier, Amsterdam, pp. 165–215.

Nyssen, J., Poesen, J., Moeyersons, J., Deckers, J., Haile, M., 2006. Processes and rates of rock fragment displacement on cliffs and scree slopes in an *amba* landscape, Ethiopia. Geomorphology 81, 265–275.

Olszewski, D.I., Dibble, H.L., Schurmans, U.A., McPherron, S.P., Smith, J.R., 2005. High desert paleolithic survey at Abydos, Egypt. Journal of Field Archaeology 30, 283–303.

Pelletier, J.D., 2007. Cantor set model of eolian dust deposits on desert alluvial fan terraces. Geology 35, 439–442.

Poesen, J.W., van Wesemael, B., Bunte, K., Benet, A.S., 1998. Variation of rock fragment cover and size along semiarid hillslopes: a case-study from southeast Spain. Geomorphology 23, 323–335.

Prose, D.V., Wilshire, H.G., 2000. The lasting effects of tank maneuvers on desert soils and intershrub flora. Open File Report OF 00-512, U.S. Department of the Interior U.S. Geological Survey.

Prospero, J.M., Lamb, P.J., 2003. African droughts and dust transport to the Caribbean climate change implications. Science 302, 1024–1027.

Reheis, M.C., Kihl, R., 1995. Dust deposition in southern Nevada and California, 1984–1989: relations to climate, source area, and source lithology. Journal of Geophysical Research 100, 8893–8918.

Reid, I., Frostick, L.E., 1985. Arid zone slopes and their archaeological materials. In: Pitty, A.F. (Ed.), Themes in Geomorphology. Croom Helm, London, pp. 141–157.

Said, R., 1990. Quaternary. In: Said, R. (Ed.), The Geology of Egypt. A.A. Balkema, Rotterdam, pp. 487–507.

Shahin, M., 1985. Hydrology of the Nile Basin. Elsevier, Amsterdam. 575 pp.

Smith, J.R., Giegengack, R., Schwarcz, H.P., 2004. Constraints on Pleistocene pluvial climates through stable-isotope analysis of fossil-spring tufas and associated gastropods, Kharga Oasis, Egypt. Palaeogeography, Palaeoclimatology, Palaeoecology 206, 157–175.

Spearman, C., 1904. The proof and measurement of association between two rings. American Journal of Psychology 15, 72–101.

Summerfield, M.A., 1991. Global Geomorphology. John Wiley & Sons, Inc., New York. 537 pp.
Szabo, B.J., Haynes Jr., C.V., Maxwell, T.A., 1995. Ages of Quaternary pluvial episodes determined by uranium-series and radiocarbon dating of lacustrine deposits of Eastern Sahara. Palaeogeography, Palaeoclimatology, Palaeoecology 113, 227–242.
Villa, P., 1982. Conjoinable pieces and site formation processes. American Antiquity 47, 276–290.
Ward, R.A., 1961. Desert pavement. The Compass of Sigma Gamma Epsilon 39, 3–8.
Wells, S.G., Dohrenwend, J.C., McFadden, L.D., Turrin, B.D., Mahrer, K.D., 1985. Late Cenozoic landscape evolution on lava flow surfaces of the Cima volcanic field, Mojave Desert, California. Geological Society of America Bulletin 96, 1518–1529.
Wells, S.G., McFadden, L.D., Poths, J., Olinger, C.T., 1995. Cosmogenic $^{3}$He surface-exposure dating of stone pavements: implications for landscape evolution in deserts. Geology 23, 613–616.
Wessa, P., 2008. Free Statistics Software, Office for Research Development and Education. version 1.1.22-r4, URL http://www.wessa.net/.
Wood, Y.A., Graham, R.C., Wells, S.G., 2005. Surface control of desert pavement pedologic process and landscape function, Cima Volcanic field, Mojave Desert, California. Catena 59, 205–230.
Yair, A., Lavee, H., Bryan, R.B., Adar, E., 1980. Runoff and erosion processes and rates in the Zin Valley Badlands, northern Negev, Israel. Earth Surface Processes 5, 205–225.